



Pharmacological inhibition of cathepsin S and of NSPs-AAP-1 (a novel, alternative protease driving the activation of neutrophil serine proteases)

Roxane Domain^{a,b,1}, Seda Seren^{a,b,1}, Uwe Jerke^c, Manousos Makridakis^d, Kuan-Ju Chen^e, Jérôme Zoidakis^d, Moez Rhimi^f, Xian Zhang^g, Tillia Bonvent^{a,b}, Cécile Croix^{a,b}, Loïc Gonzalez^{a,b}, Dedong Li^e, Jessica Basso^e, Christophe Paget^{a,b}, Marie-Claude Viaud-Massuard^{a,b}, Gilles Lalmanach^{a,b}, Guo-Ping Shi^h, Ali Aghdassiⁱ, Antonia Vlahou^d, Patrick P. McDonald^e, Isabelle Couillin^j, Rich Williams^k, Ralph Kettritz^{c,1}, Brice Korkmaz^{a,b,*}

^a INSERM UMR-1100, Research Center for Respiratory Diseases, Tours, France

^b Université de Tours, Tours, France

^c Experimental and Clinical Research Center, Charité und Max-Delbrück-Centrum für Molekulare Medizin in der Helmholtz-Gemeinschaft (MDC), Berlin, Germany

^d Biotechnology Division, Biomedical Research Foundation, Academy of Athens, Athens, Greece

^e Research Department, Insmad Incorporated, Bridgewater, NJ, USA

^f INRAE UMR-1319, Microbiota Interaction with Human and Animal Team (MIHA), Micalis Institute, AgroParisTech, Université Paris-Saclay, Jouy-en-Josas, France

^g School of Food and Biological Engineering, Hefei University of Technology, Hefei, Anhui, China

^h Department of Medicine, Cardiovascular Medicine, Brigham and Women's Hospital and Harvard Medical School, Boston, MA, USA

ⁱ Department of Medicine A - Gastroenterology, Nephrology, Endocrinology and Rheumatology, University Medicine Greifswald, Greifswald, Germany

^j CNRS UMR-7355, Experimental and Molecular Immunology and Neurogenetics, Université d'Orléans, Orleans, France

^k The Patrick G Johnston Center for Cancer Research, Queen's University, Belfast, UK

¹ Nephrology and Intensive Care Medicine, Charité-Universitätsmedizin, Berlin, Germany

ARTICLE INFO

Keywords:

Cathepsin C
Cysteine cathepsin
Neutrophil serine protease
Zymogen
Synthetic inhibitor
Therapeutic approach

ABSTRACT

An uncontrolled activity of neutrophil serine proteases (NSPs) contributes to inflammatory diseases. Cathepsin C (CatC) is known to activate NSPs during neutrophilic differentiation and represents a promising pharmacological target in NSP-mediated diseases. In humans, Papillon-Lefèvre syndrome (PLS) patients have mutations in their *CTSC* gene, resulting in the complete absence of CatC activity. Despite this, low residual NSP activities are detected in PLS neutrophils (<10% vs healthy individuals), suggesting the involvement of CatC-independent proteolytic pathway(s) in the activation of proNSPs. This prompted us to characterize CatC-independent NSP activation pathways by blocking proCatC maturation. In this study, we show that inhibition of intracellular CatS almost completely blocked CatC maturation in human promyeloid HL-60 cells. Despite this, NSP activation was not significantly reduced, confirming the presence of a CatC-independent activation pathway involving a CatC-like protease that we termed NSPs-AAP-1. Similarly, when human CD34⁺ progenitor cells were treated with CatS inhibitors during neutrophilic differentiation *in vitro*, CatC activity was nearly abrogated but ~30% NSP activities remained, further supporting the existence of NSPs-AAP-1. Our data indicate that NSPs-AAP-1 is a cysteine protease that is inhibited by reversible nitrile compounds designed for CatC inhibition. We further established a proof of concept for the indirect, although incomplete, inhibition of NSPs by pharmacological targeting of CatC maturation using CatS inhibitors. This emphasizes the potential of CatS as a therapeutic target for inflammatory

Abbreviations: α 1PI, alpha1-protease inhibitor; ABZ, *ortho*-aminobenzoic acid; ACT, alpha1-antichymotrypsin; ANCA, anti-neutrophil cytoplasmic autoantibody; BCA, bicinchoninic acid; CatC, cathepsin C; CatG, cathepsin G; DMSO, dimethyl sulfoxide; ECL, enhanced chemiluminescence; EDDnp, *N*-(2,4-dinitrophenyl)ethylenediamine; FRET, fluorescence resonance energy transfer; GPA, granulomatosis with polyangiitis; HBSS, Hank's balanced salt buffer; hNE, human neutrophil elastase; HSC, hematopoietic stem cell; MPO, myeloperoxidase; NETs, neutrophil extracellular traps; NSP, neutrophil serine protease; PBS, phosphate-buffered saline; PLS, Papillon-Lefèvre syndrome; PR3, proteinase 3; PR3^m, membrane-bound PR3; RT, room temperature; SDS-PAGE, sodium dodecyl sulfate polyacrylamide gel electrophoresis; WBC, white blood cell.

* Corresponding author at: INSERM UMR-1100 "Research Center for Respiratory Diseases" and Université de Tours, Tours, France.

E-mail address: brice.korkmaz@inserm.fr (B. Korkmaz).

¹ Equal contribution

<https://doi.org/10.1016/j.bcp.2024.116114>

Received 9 November 2023; Received in revised form 14 February 2024; Accepted 5 March 2024

Available online 16 September 2024

0006-2952/© 2024 The Author(s). Published by Elsevier Inc. This is an open access article under the CC BY-NC license (<http://creativecommons.org/licenses/by-nc/4.0/>).

diseases. Thus, preventing proNSP maturation using a CatS inhibitor, alone or in combination with a CatC/NSPs-AAP-1 inhibitor, represents a promising approach to efficiently control the extent of tissue injury in neutrophil-mediated inflammatory diseases.

1. Introduction

Neutrophils are the first line of cellular defense against invading pathogens and play an important role in the inflammatory response. They are differentiated from hematopoietic stem cells in the bone marrow and mature neutrophils are released into the blood in humans. Neutrophils mount several functional responses to eliminate pathogens. In addition to phagocytosis, these responses include the secretion of cytotoxic molecules such as neutrophil serine proteases (NSPs) – neutrophil elastase (NE), proteinase 3 (PR3), cathepsin G (CatG), and NSP4; the generation of reactive oxygen species (ROS); and the extrusion of web-like structures of decondensed chromatin decorated with numerous microbicidal proteins, called NETs (for neutrophil extracellular traps) [1]. NSP-mediated proteolysis is controlled endogenously by proteins of the serpin superfamily (including α 1-protease inhibitor (α 1PI) and α 1-antichymotrypsin) as well as by canonical inhibitors such as secretory leukocyte peptide inhibitor (SLPI) and elafin [2,3]. Conversely, dysregulation of NSP activity contributes to the pathogenesis of neutrophil-mediated chronic inflammatory and auto-immune diseases [2,3].

NSPs are synthesized as inactive zymogens (proNSPs) containing an N-terminal two-residue propeptide, which maintains the zymogen in an inactive conformation. Activation of NSP zymogens occurs through the removal of the N-terminal dipropeptide by a cysteine protease called cathepsin C (CatC, EC 3.4.14.1; also known as dipeptidyl peptidase 1/DPP1) [4]. CatC is a highly conserved lysosomal dipeptidyl aminopeptidase belonging to the C1 family (clan CA) of cysteine peptidases [5,6]. Eleven cysteine cathepsins that are closely related to papain have been identified in humans [7]. All of them are synthesized as inactive preproenzymes containing a signal peptide, a propeptide, and a catalytic domain; the latter corresponding to the mature proteolytically active form [8,9]. Although most of human cysteine cathepsins are endopeptidases, CatB, C, H, and X retain an exopeptidase activity driven by their structural characteristics and are not auto-catalytically activated [7,9–11]. Unlike other cysteine cathepsins, CatC possesses a N-terminal exclusion domain responsible for its diaminopeptidase activity [5], allowing activation of NSP zymogens.

CatC is initially synthesized as a 55-kDa monomeric single chain proenzyme. Newly synthesized monomers associate to form proCatC dimers which undergo proteolytic cleavage at several sites to release internal 10-kDa propeptides and finally associate to form a functional tetramer [12]. Human proCatC is not auto-catalytically processed *in vitro* but is instead matured by CatL-like proteases [13]. These proteases process proCatC in two consecutive steps. The first one releases the exclusion domain along with two peptides of 36 and 33 kDa, each one composed of the truncated propeptide, and the heavy and light chains. The second step involves the release of the heavy chain from each peptide [14–16]. Each mature CatC monomer in the functional tetramer consists of three subunits associated by non-covalent interactions, a 16-kDa N-terminal “exclusion” domain, a 23-kDa heavy chain and a 7.5-kDa light chain [14], with the heavy and the light chains forming a papain-like structure. The best characterized physiological function of active CatC is the activation of pro-inflammatory granular serine proteases of immune cells, including the NSPs [17].

A genetic defect in the *CTSC* gene (which encodes CatC) causes Papillon-Lefèvre syndrome (PLS, OMIM: 245000) or Haim-Munk syndrome in humans [18]. In our previous studies, we investigated the stability of mutated CatC in PLS white blood cells, neutrophils [19] and urines [20]. Nonsense, frameshift and missense mutations all resulted in a total absence of CatC protein in PLS patients [19,20]. Whereas

nonsense and frameshift mutations are expected to affect the expression of mutated CatC, it is surprising for missense mutations to alter the stability of mutated proteins. It has been suggested that the latter mutations induce the intracellular proteolytic degradation of CatC [20,21]. In any event, the loss of CatC activity in neutrophils from PLS patients is associated with a strong reduction in NSP proteolytic activities but leaves significant residual activities (<10 % vs healthy individuals) [19,22] (Fig. 1). This suggests that CatC is the major, but not unique, protease involved in the activation of proNSPs [19]. In spite of their deficiency in CatC, PLS patients do not present marked immunodeficiency. This provided the rationale for a transient pharmacological inhibition of CatC activity in precursor cells within the bone marrow as a therapeutic strategy to regulate NSP activity in inflammatory and/or immune disorders [2,13,23].

Pharmacological inhibition of CatC can be achieved either using chemical inhibitors interacting with the mature, functional protease (*direct inhibition*) [24,25], or by impairing the activation of its proform by targeting proCatC-converting protease(s) (*indirect inhibition*) [15]. Potent reversible CatC inhibitors (**IcatC_{XPZ-01}** [25], **BI-9740** [26], **BI-1291583** [27], **brensocatib** [28,29] and **HSK31858** [30]) as well as irreversible CatC inhibitors (**GSK2793660** [31] and compound **22** [32]) have been synthesized, some of which are now being tested preclinically and in clinical trials [13,33,34] in patients with non-cystic fibrosis bronchiectasis, cystic fibrosis or chronic rhinosinusitis without nasal polyps (CRSsNP) [35].

Our previous work showed that PLS neutrophils display incompletely suppressed NSP activities despite a loss-of-function CatC mutation [19], which indicates that NSP-driven tissue damage might not be abrogated by blocking CatC alone. Importantly, our findings also suggested the existence of NSPs alternative activating protease(s) (NSPs-AAPs), which should ideally be targeted, along with CatC, to bring about full NSP inhibition. In this study, we investigated the proteolytic processes involved in the generation of active NSPs to generate further experimental evidence of the existence of NSPs-AAP(s), and to identify new therapeutic targets for NSP-mediated inflammatory diseases. To this end, we employed different pharmacological approaches to block pro-CatC maturation. We first used potent, cell-permeable inhibitors and determined the fate of proNSPs in a human promyeloid cell line as well as in neutrophils generated from human hematopoietic stem cells. We then investigated the proteolytic pathways involved in the activation of murine NSPs to understand the pharmacodynamics of CatC inhibitors.

2. Materials and methods

2.1. Materials

Substrates: Gly-Phe-AMC (#AMC-033) and Gly-Arg-AMC (#AMC-031) were from MP Biomedicals (Illkirch, France), ABZ-VAD(nor) VADYQ-EDDnp [36,37], Abz-APQIMDDQ-EDDnp [36,37], Abz-TPFSGQ-EDDnp [38], Abz-VARCADYQ-EDDnp were from GeneCust (Boynes, France). **Inhibitors:** **E64d** (2S,3S-trans-(Ethoxycarbonyloxirane-2-carbonyl)-L-leucine-(3-methylbutyl) amide; aloxistatin) (HY-100229) was from MedChemExpress (Sollentuna, Sweden), compound **1** (calpain inhibitor VI, N-(4-fluorophenylsulfonyl)-L-valyl-L-leucinal) (sc-293979); compound **2** (calpeptin, N-benzyloxycarbonyl-L-leucyl-nor-leucinal) (sc-202516); compound **3** (N-Acetyl-L-leucyl-L-leucyl-L-methioninal) (sc-201268), compound **4** (Z-L-Abu-CONH-ethyl) (sc-301995) and **PD 150606** (3-(4-Iodophenyl)-2-mercapto-(Z)-2-prope-noic Acid) (sc-222133) were from Santa Cruz Biotechnology (Heidelberg Germany). **RO5461111** (**IcatS_{RO-11}**) was provided by Roche Pharma

Research & Early Development, Roche Innovation Center Basel (Basel, Switzerland). Compound **22** (**IcatC_{EGFR-22}**) was kindly provided by Dr Zhiyuan Zhang (National Institute of Biological Sciences (NIBS), China). **IcatC_{XPZ-01}** was synthesized as in Guarino et al., [39]. **BI-9740** (**IcatC_{BI-9740}**) was obtained via Boehringer Ingelheim's innovation platform OpnMe (<https://opnme.com>) [40]. **GSK2793660** (**IcatC_{GSK-60}**) was generously provided by Dr Aili Lazaar from GlaxoSmithKline Pharmaceuticals (Brentford, UK). (L)-Thi-(L)-Phe-CN was generously provided by Dr Adam Lesner (University of Gdansk/Poland), Biotin-Pro-Tyr-Asp-Ala^P(O-C₆H₄-4-Cl)₂ was synthesized as in Guarino et al., [39]. Alpha-1-antitrypsin (16-16-011609) and alpha-1-antichymotrypsin (16-16-012400) were from Athens Research & Technology (Athens, Georgia, USA). **Proteases**: mature human CatC was from Unizyme Laboratories (Hørsholm, Denmark). Active human PR3 and NE were from Athens Research & Technology (Athens, Georgia, USA). Active Human CatS and CatG were from Millipore (Molsheim, France). Recombinant human CatL (952CY) was from R&D system (Lille, France) and CatL from human liver (219402) was from Calbiochem® (San Diego, California, USA). **Antibodies**: murine anti-human CatC antibody directed against the heavy chain of CatC [15] (sc-74590), rabbit anti-human MPO antibody directed against the heavy chain (C-16-R, sc-16128-R) and rabbit anti-mouse CatG (sc-33207) were purchased from Santa Cruz Biotechnology (Heidelberg, Germany). Goat anti-human CatS antibody (AF1183) and goat anti-human CatL (AF952) were purchased from R&D system (Lille, France). Rabbit anti-human PR3 [15] (ab133613), rabbit anti-mouse NE antibody (ab68672) and rabbit anti-human CatD (ab75852) were purchased from Abcam (Cambridge, UK). Rabbit anti-human CatG (83578S) and rabbit anti-human NE (63610S) were purchased from Cell Signaling (Beverly, Massachusetts, USA). Murine anti-human β-actin antibody (A2228), peroxidase conjugated rabbit anti-goat IgG antibody (A5420) and peroxidase conjugated sheep anti-mouse IgG antibody (A5906) were purchased from Sigma-Aldrich (Saint-Quentin Fallavier, France). Peroxidase conjugated goat anti-rabbit IgG (H + L) antibody (Affini pure) (111-035-003) was purchased from Jackson ImmunoResearch (Cambridgeshire, UK).

2.2. Synthesis of IcatS_{#54}

Boc-Cys-OMe was alkylated under standard basic conditions, followed by removal of Boc protecting group to afford **1**. A one pot two-step

reductive amination reaction was conducted to install the tri-fluormethylamino amide isostere. The intermediate acid was then oxidised to the sulfone-acid **2**. The acid **2** was coupled to the 4,4-disubstituted piperidine under standard conditions to afford compound **3** (**IcatS_{#54}**). Reagents: (a) 2-fluorobenzyl bromide, K₂CO₃, DMF, 20 h; (b) 4 N HCl dioxane, 1 h; (c) (i) 4-Fluorotrifluoroacetophenone, K₂CO₃, MeOH, 50 °C, 18 h; (ii) Zn(BH₄)₂, DME, ACN, -40 °C, 4 h; (d) NaTg, TBAH, H₂O₂, EtOAc, 3 h; (e) 4-amino-4-Cyano-N-Me-piperidine, HATU, NMM, DMF, 18 h (Fig. 2).

2.3. IC₅₀ determination

Serial dilutions (0–50 μM for compound **1**, **IcatS_{#54}** and 0–0.5 μM for compound **2**) were made in assay buffer in presence of recombinant cysteine proteases at 2 nM (CatB, C, F, K, L, S and V). After 15 min of incubation at 37 °C under low agitation, fluorogenic substrate was added (Gly-Phe-AMC for CatC, Z-Leu-Arg-AMC for CatS and Z-Phe-Arg-AMC for other cysteine cathepsins, 20 μM for each substrate). IC₅₀ values were derived by a sigmoidal dose–response (variable slope) curve using GraphPad Prism software. The reported data are average of at least three independent experiments in duplicate.

2.4. Blood neutrophil purification

Blood from healthy volunteers from the EFS (Etablissement Français du Sang) and blood from PLS patients (Germany) were collected in EDTA tubes. Neutrophils were isolated from blood using EasySep™ Direct Human Neutrophil Isolation Kit (StemCell Technologies (19666), Saint Égrève, France). This kit isolates neutrophils directly from human whole blood by immunomagnetic negative selection. Unwanted cells are labeled with antibodies EasySep™ Direct RapidSpheres™ and separated using an EasySep™ magnet. Once collected neutrophils were washed with PBS and lysed in 50 mM HEPES buffer, 750 mM NaCl, 0.1 % Nonidet P-40 (NP-40), pH 7.4. Soluble fractions were separated from cell debris by centrifugation at 10,000g for 20 min. Proteins were assayed with a bicinchoninic acid assay (BCA) (23227, Thermo Fisher Scientific, Villebon sur Yvette, France).

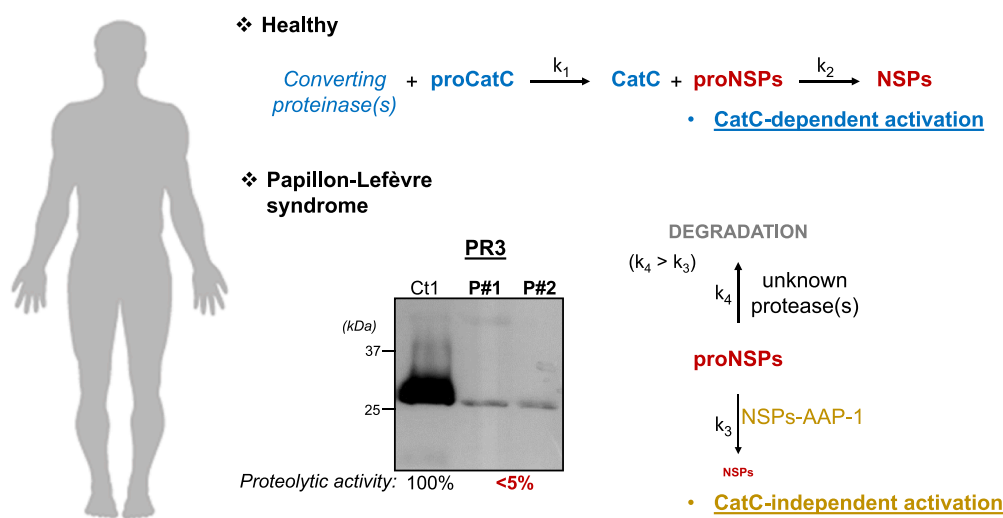


Fig. 1. ProNSP processing pathways in human. Characterization of NSPs in neutrophils from PLS patients with CatC deficiency allowed the highlighting of a CatC independent processing and activating pathway (k₃) catalyzed by unknown protease(s) [19], called NSPs-AAP-1 in this study. Little amounts of synthesized proNSPs are activated while the rest are eliminated during neutrophil differentiation. The differentiation of isolated human bone-marrow neutrophilic precursors in presence of the cell-permeable CatC inhibitor **IcatC_{XPZ-01}** allowed the highlighting of a proteolytic processing pathway (k₄) catalyzed by unknown protease(s) in granules [39] responsible for the elimination of NSP zymogens. However, there is no evidence showing that k₃ and k₄ exist in healthy neutrophilic precursors containing proteolytically active CatC.

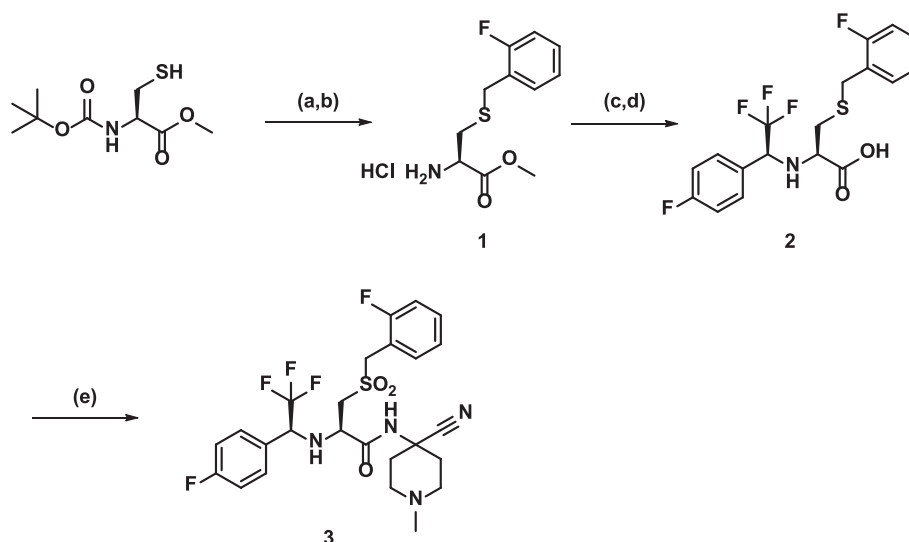


Fig. 2. Synthetic schema for the synthesis of **IcatS**_{#54}.

2.5. Proteomics and bioinformatics analysis of HL-60 cells

HL-60 cells were cultured in RPMI-1640 GlutaMAX™ supplement (61870044, Gibco™) medium supplemented with 10 % FBS (Fetal Bovine Serum substitute, Fetal + Triple 0.1 μm Sterile Filtered, SER-ANA®, S-FBSP-EU-015), 50 units/ml penicillin and 50 μg/ml streptomycin at 37 °C in a humidified atmosphere containing 5 % CO₂ (passage number < 30). Cell pellets were homogenized in FASP (Filter Aided Sample Preparation) lysis buffer (4 % SDS, 0.1 M DTE, 0.1 M Tris-HCl pH 7.6). Protein concentration was determined by Bradford assay. Protease inhibitors (Roche, Basel, Switzerland) were added at a final concentration of 3.6 % and samples were stored at -80 °C until further use. Protein extracts (200 μg/sample) were processed using filter aided sample preparation (FASP) as described previously [41], with minor modifications [42]. Briefly, buffer exchange was performed in Amicon Ultra Centrifugal filter devices (0.5 ml, 30-kDa MWCO; Merck) at 14,000 rcf for 15 min at room temperature. The protein extract was mixed with urea buffer (8 M urea in 0.1 M Tris-HCl, pH 8.5) and centrifuged. The concentrate was diluted with urea buffer and centrifugation was repeated. Alkylation of proteins was performed with 0.05 M iodoacetamide in urea buffer for 20 min in the dark followed by a centrifugation at 14,000 rcf for 10 min at RT. Additional series of washes were conducted with urea buffer (2 times) and ammonium bicarbonate buffer (50 mM NH₄HCO₃, pH 8.5, 2 times). Tryptic digestion was performed overnight at RT in the dark, using a trypsin to protein ratio of 1:100. Peptides were eluted by centrifugation at 14,000 rcf for 10 min, lyophilized and stored at -80 °C until further use.

LC-MS/MS experiments were performed on the Dionex Ultimate 3000 UHPLC system coupled with the high-resolution nano-ESI QExactive HF mass spectrometer (Thermo Scientific). Each sample was reconstituted in 200 μL loading solution composed of 0.1 % v/v formic acid. A 5 μL volume was injected and loaded on the Acclaim PepMap 100 (100 μm × 2 cm C18, 5 μm, 100 Å) trapping column with the loading pump operating at a flow rate of 5 μL/min. For the peptide separation the Acclaim PepMap RSLC, 75 μm × 50 cm, C18, 2 μm, 100 Å column was used for multi-step gradient elution. Mobile phase (A) was composed of 0.1 % formic acid and mobile phase (B) was composed of 100 % acetonitrile, 0.1 % formic acid. The peptides were eluted under a 240 min gradient from 2 % (B) to 80 % (B). Flow rate was 300 nL/min and column temperature was set at 35 °C. Gaseous phase transition of the separated peptides was achieved with positive ion electrospray ionization applying a voltage of 2.5 kV. For every MS survey scan, the top 10 most abundant multiply charged precursor ions between *m/z*

ratio 300 and 2200 and intensity threshold 500 counts were selected with FT mass resolution of 70,000 and subjected to HCD fragmentation. Tandem mass spectra were acquired with FT resolution of 35,000. Normalized collision energy was set to 33 and already targeted precursors were dynamically excluded for further isolation and activation for 30 sec with 5 ppm mass tolerance.

Raw files were analysed with Proteome Discoverer 1.4 software package (Thermo Finnigan), using the Sequest search engine and the Uniprot human (Homo sapiens) reviewed database, including 20,204 entries. The search was performed using carbamidomethylation of cysteine as static and oxidation of methionine as dynamic modifications. Two missed cleavage sites, a precursor mass tolerance of 10 ppm and fragment mass tolerance of 0.05 Da were allowed. False discovery rate (FDR) validation was based on *q* value: target FDR: 0.01.

Label free quantification was performed by utilizing the precursor ion area values exported from the total ion chromatogram as defined by the Proteome Discoverer 1.4 software package. Output files from Proteome Discoverer were processed with R programming language for statistical computing (version 4.0.3). Raw protein intensities for each sample were subjected to normalization according to $X' = X/\text{Sum}(X_i) \times 10^6$.

2.6. Inhibition of proteases in HL-60 cells and human CD34⁺-derived neutrophils

HL-60 cells ($2\text{--}3 \times 10^6$ cells) were cultured for 72 h and treated with **E64d** (1, 10, 100 μM). Continuous inhibition of CatS was maintained in cell cultures (starting at $2\text{--}3 \times 10^6$ cells) with the synthetic inhibitors **IcatS**_{#54} ((*R*)-*N*-(4-cyano-1-methylpiperidin-4-yl)-3-((2-fluorobenzyl)sulfonyl)-2-(((*S*)-2,2,2-trifluoro-1-(4-fluorophenyl)ethyl)amino)propanamide), **IcatS**_{RO-11} ((2*S*,4*R*)-*N*-(1-cyanocyclopropyl)-4-((4-(2-methylpyridin-4-yl)-2-(trifluoromethyl)phenyl)sulfonyl)-1-(1-(trifluoromethyl)cyclopropane-carbonyl)pyrrolidine-2-carboxamide), **IcatS** (*N*-(1-cyanocyclopropyl)-3-((2,3-difluorobenzyl)sulfonyl)-2-((2,2,2-trifluoro-1-(4-fluorophenyl)ethyl)amino)propanamide), compound **1** (2*S*-[[[(4-fluorophenyl)sulfonyl]amino]-*N*-[(1*S*)-1-formyl-3-methylbutyl]-3-methylbutanamide), compound **2** (calpeptin, *N*-benzylloxycarbonyl-L-leucyl-norleucinal), compound **3** (*N*-Acetyl-L-leucyl-L-leucyl-L-methioninal or compound **4** (*Z*-L-Abu-CONH-ethyl). Continuous direct inhibition of CatC was maintained in cell cultures (starting at $2\text{--}3 \times 10^6$ cells) with the synthetic inhibitors **IcatC**_{XPZ-01} (1 μM), **IcatC**_{GSK-60} (10 μM) or **IcatC**_{EGFR-22} (0.2 μM). Either compounds **1**, compounds **4**, or **IcatS**_{#54} (10 μM) was supplemented with the CatC

inhibitor, **IcatC_{XPZ-01}** (1 μ M) or **IcatC_{GSK-60}** (10 μ M).

Umbilical cord blood samples were taken giving informed consent (Ethics vote EA4/025/18). Mononuclear cells were obtained from anti-coagulated cord blood by centrifugation over a LSM1077 (PAA, Pasching, Austria) gradient at $800 \times g$ for 20 min. Cells were washed and stained using the CD34⁺ progenitor isolation kit (Miltenyi, Bergisch-Gladbach, Germany) and sorted according to the manufacturer's instructions. CD34⁺ cells were cultivated in stem span serum free medium (Cell Systems, St. Katharinen, Germany) supplemented with Penicillin/Streptomycin, 100 ng/ml SCF, 20 ng/ml TPO and 50 ng/ml FLT3-L (Peprotech, London, UK) for expansion. Neutrophil differentiation was performed in RPMI with 10 % FCS, 10 ng/ml G-CSF (Peprotech), and either DMSO control, **IcatS_{#54}** (20 μ M) or compound **1** (10 μ M and 30 μ M). **IcatS_{#54}** and compound **1** were supplemented with **IcatC_{XPZ-01}** (1 μ M) and **IcatC_{BL-9740}** (1 μ M). Medium was changed every other day. We PR3-phenotyped the neonatal neutrophils obtained from the freshly harvested umbilical cords by flow cytometry prior to the CD34⁺ HSC isolation. We selected only cord blood where the neonatal neutrophils showed a clear bimodal membrane PR3 pattern.

HL-60 cells were lysed in 50 mM HEPES buffer, 750 mM NaCl, 0.1 % Nonidet P-40 (NP-40), pH 7.4. Soluble fractions were separated from cell debris by centrifugation at $10,000 \times g$ for 20 min. CD34⁺ or neutrophil-differentiated CD34⁺ HSC were lysed in 50 mM HEPES buffer, 750 mM NaCl, 0.05 % NP-40, pH 7.4. Soluble fractions were separated from cell debris by centrifugation at $10,000 \times g$ for 20 min and then concentrated by ultrafiltration (Vivaspin (filtration threshold 10-kDa)) in some experiments. Proteins were assayed with a BCA.

2.7. Animal experiments

All studies were carried out under approval of: 1. "Comité d'Ethique Appliqué à l'Expérimentation Animale" under the protocols No.: #12504-201720818404277v1, #201604071220401-4885 and #1728), 2. the Care and Use of Laboratory Animals published by the US National Institutes of Health and were approved by the Harvard Medical School Standing Committee on Animals (Protocol No.: #2016N000442). 3. the Institutional Animal Care and Use Committee (IACUC) of Rutgers University Animal Care Committee (Protocol No.: PROTO999900342). Wild-type (WT) male C57BL/6 mice were purchased from Jackson Laboratories, (Bar Harbor, ME) or Janvier Labs (Le Genest-Saint-Isle, France), *Ctsc*^{-/-} and NSP triple knock-out mice on C57BL/6 genetic background were obtained from Washington University (Dr C. Pham) and bred at Charles River Laboratories (Wilmington, MA). The mice used in this study were 11–16 weeks old. Prolonged **IcatC_{XPZ-01}** administration was performed as in [39].

2.8. Murine neutrophils differentiation from bone marrow progenitor cells and inhibition of intracellular proteases

WT (n = 5) and *Ctsc*^{-/-} (n = 5) femurs and tibias of both hind limbs were harvested for each animal. The bones were kept on wet ice until processing for bone marrow collection. In brief, bone cutters were used to cut off the epiphysis of the long bones to expose the bone marrow-filled cavity. Each bone cavity was then flushed with 5 ml/bone of PBS through a 40- μ m cell strainer and collected in a 50-ml conical tube. Cells were spun down ($400 \times g$, 4 °C, 5 min) and the supernatants were discarded.

For mixed white blood cells (WBC) sample preparation, the bone marrow cells were lysed with 1X red blood cell (RBC) lysis buffer (Sigma R7757) at room temperature for 2 min, followed by the addition of 10 ml PBS to stop RBC lysis. The cell suspension was centrifuged ($400 \times g$, 4 °C, 5 min), resuspended in 1 ml in PBS, and centrifuged ($400 \times g$, 4 °C, 5 min).

For promyelocytes preparation, bone marrow promyelocytes were isolated using Direct Lineage Cell Depletion Kit (Miltenyi, 130–110-470). This kit isolates untouched lineage-negative cells from mouse bone

marrow cell suspension using microbeads conjugated to monoclonal antibodies against mature hematopoietic cells, the marked cells are retained in a LS column (Miltenyi, 130–042-401) fixed on a magnet and untouched cells are collected. Briefly, cells were counted and resuspended in ice-cold MACS buffer (pH 7.2 PBS plus 0.5 % BSA and 2 mM EDTA), 80 μ L of buffer per 2×10^7 total cell. Followed by 20 μ L per 2×10^7 total cell of Direct Lineage Cell Depletion Cocktail. The mixture was then incubated for 10 min at 2–8 °C. The cell suspension was applied to the Magnetic separation LS Column (MACS, Miltenyi, 130 042 401). Unlabeled cells representing the enriched promyelocytes were collected from the flow-through. The column was washed with 3 ml of ice-cold MACS buffer three times.

Collected cells were cultured at 200,000 cells/ml in IMDM medium, supplement GlutaMAX™, HEPES (Gibco™, 31980030), 10 % FBS (SERANA®, S-FBSP-EU-015), 1 % Pen Strep (Penicillin Streptomycin, Gibco™, 151–40-122) with 50 ng/ml of Stem cell factor (Recombinant mouse SCF carrier free, BioLegend®, 579704) and 50 ng/ml of Interleukin-3 (Recombinant mouse IL-3 carrier free, BioLegend®, 575504) supplemented or not with chemical inhibitor (**IcatC_{XPZ-01}** (1 μ M)) for 3 days. At day 3 cells were counted and resuspended at 200,000 cells/ml with the same medium with 50 ng/ml of SCF, IL-3 and Granulocyte Colony Stimulating Factor (Recombinant mouse G-CSF carrier free, BioLegend®, 574604) and cultured for two days. At day 5 same method were used than at day 3 but medium was supplemented with only 50 ng/ml of G-CSF. At day 7 cells were washed and counted, some of them will be used for FACS analysis and the rest will be lysed. FACS analysis were used to control neutrophil population. Cells were marked with antibodies against CD45 (APC/Cyanine7 anti-mouse CD45, BioLegend®, 103116), Ly6G (FITC anti-mouse Ly6G, BioLegend®, 127606), CD11b (PE/Cy7 anti-mouse/human CD11b, BioLegend®, 101216) and Live/Dead™ (Live/Dead™ Fixable Aqua Dead Cell Stain Kit, Invitrogen, L34957).

Cells were lysed in 50 mM HEPES buffer, 750 mM NaCl, 0.1 % NP-40, pH 7.4. Soluble fractions were separated from cell debris by centrifugation at $15,000 \times g$ for 20 min.

2.9. Total protein quantification

The Pierce™ BCA Protein Assay Kit (Thermo Scientific, 23227) was used to measure the total protein of the samples after lysis to allow for subsequent normalization, following the manufacturer's instructions.

2.10. Measurements of protease activities in cell lysates

In HL-60 cells, CD34⁺ or neutrophil-differentiated CD34⁺ HSC lysates, proteolytic activities of CatC and NSPs were measured as in [15]. Briefly, the CatC activity in cell lysates was measured spectrofluorometrically (Spectra Max Gemini EM) at 460 nm (excitation: 350) with or without the nitrile inhibitor (L)-Thi-(L)-Phe-CN using Gly-Phe-AMC (20 μ M final) as substrate in 50 mM sodium acetate, 30 mM NaCl, 1 mM EDTA, 2 mM DTT, pH 5.5 at 37 °C. The PR3 activity in cell lysates was measured at 420 nm (excitation: 320) with or without the PR3 inhibitor Bt-PYDnV^P(O-C₆H₄-4-Cl)₂ (nV: norvaline) (1 μ M in 50 mM HEPES buffer, 750 mM NaCl, 0.05 % NP40, pH 7.4 at 37 °C) using Abz-VADnVADYQ-EDDnp (20 μ M) as substrate. CatG activity was measured at 420 nm (excitation: 320) in 50 mM HEPES buffer, 100 mM NaCl, 0.05 % NP 40, pH 7.4 at 37 °C, in the presence or not of 1 μ M anti-chymotrypsin, using Abz-TPFSGQ-EDDnp (20 μ M) as substrate. NE activity was measured at 420 nm (excitation: 320) with or without the NE inhibitor Epi-hNE-4 (1 μ M in 50 mM HEPES buffer, 750 mM NaCl, 0.05 % NP40, pH 7.4 at 37 °C) using Abz-APQQIMDDQ-EDDnp (20 μ M) as substrate.

In murine neutrophils differentiated from bone marrow progenitor cells lysates and bone marrow lysates CatC activity was measured in activity buffer (50 mM sodium acetate, 30 mM NaCl, 1 mM EDTA, 2 mM DTT, pH 5.5 at 37 °C) at 460 nm (excitation: 350) with or without the

nitrile inhibitor (L)-Thi-(L)-Phe-CN using Gly-Arg-AMC (20 μ M) as substrate. Activity of NE was measured with a fluorogenic substrate in activity buffer (50 mM HEPES buffer, 750 mM NaCl, 0.05 % NP40, pH 7.4) at 37 °C with or without the inhibitor α 1PI (1 μ M) at 420 nm (excitation: 320) using Abz-APQQIMDDQ-EDDnp as substrate, PR3 activity was measured in the same conditions using Abz-VARCADYQ-EDDnp as substrate. CatG activity was measured in the same conditions as above.

2.11. Western blotting

The pellet of CD34⁺ HSC or neutrophil-differentiated CD34⁺ HSC were lysed in sample buffer (20 mM Tris (pH 8,8), 138 mM NaCl, 10 % glycerol, 2 mM EDTA, 1 % Triton-X-100, 1 % NP-40 and protease inhibitor mix). The total protein concentration has been determined by the BCA (Thermo Fisher Scientific, Villebon sur Yvette, France) or Bradford (Bio-Rad, Hercules, USA) assay. HL60 cells lysates, and CD34⁺ samples were separated by SDS-PAGE under denaturing/reducing conditions and transferred to Hybond-ECL membranes. Free sites were saturated by incubation in PBS, 0.1 % Tween-20, 5 % fat-free milk for 1 h and the membranes were then incubated with goat anti-human CatS antibody (diluted 1:1000), murine anti-human CatC antibody directed against the heavy chain of CatC (diluted 1:1000), rabbit anti-human PR3 [15] (diluted 1:1000), rabbit anti-human CatG (diluted 1:1000), rabbit anti-human NE (diluted 1:1000) or goat anti-human CatL (diluted 1:1000), in PBS, 0.1 % Tween-20, 5 % non-fat milk overnight at 4 °C. The membranes were washed three times in PBS, 0.1 % Tween-20, incubated for 1 h30 with a peroxidase-coupled secondary antibody diluted 1:10000 or 1:5000 in PBS, 0.1 % Tween-20 5 % non-fat milk. For loading control, membranes were stripped with H₂O₂ 35 % for 20 min at 37 °C. Then incubated with murine anti-human β -actin antibody (diluted 1:1000) or rabbit anti-human MPO antibody directed against the heavy chain (diluted 1:1000) in PBS, 0.1 % Tween-20, 5 % non-fat milk overnight at 4 °C. The membranes were washed three times in PBS, 0.1 % Tween-20, incubated for 1 h30 with a peroxidase-coupled secondary antibody (diluted 1:5000) in PBS, 0.1 % Tween-20, 5 % non-fat milk.

Murine neutrophils differentiated from bone marrow progenitor cells lysates and bone marrow lysates were treated as above and incubated with murine anti-human CatC antibody (diluted 1:1000), rabbit anti-mouse CatG (diluted 1:500), or rabbit anti-mouse NE antibody (diluted 1:1000) in PBS, 0.1 % Tween-20, 5 % non-fat milk overnight at 4 °C. The membranes were washed three times in PBS, 0.1 % Tween-20, incubated for 1 h30 with a peroxidase-coupled secondary antibody (diluted 1:5000) in PBS, 0.1 % Tween-20, 5 % non-fat milk. For loading control, membranes were stripped with H₂O₂ 35 % for 20 min at 37 °C. Then incubated with rabbit anti-human MPO antibody directed against the heavy chain (diluted 1:1000) in PBS, 0.1 % Tween-20, 5 % non-fat milk overnight at 4 °C. The membranes were washed three times in PBS, 0.1 % Tween-20, incubated for 1 h30 with a peroxidase-coupled secondary antibody (diluted 1:5000) in PBS, 0.1 % Tween-20, 5 % non-fat milk.

3. Results

3.1. ProCatC-converting proteases in human promyelocytic HL-60 precursor cells

We first aimed to identify candidate cysteine proteases that could activate proCatC in HL-60 cells, by immunoblot analysis. CatF, CatK or CatV were not detectable in concentrated cell-free supernatants or in cell lysates (*data not shown*). By contrast, HL-60 cells mainly secreted ~ 42-kDa proCatL whereas the cell lysates contained only the propeptide lacking the ~ 32-kDa single chain of mature CatL (Fig. 3A). Furthermore, HL-60 cells secreted similar amounts of 32-kDa proCatS and ~ 23-kDa mature CatS, whereas the cell lysates contained mainly mature CatS (Fig. 3B). We next broadened our scope and analyzed the entire HL-60

cell proteome, using a mass spectrometry-based proteomic approach. Among the 3693 proteins that were identified [43] (*Data reference*), CatS was the only proCatC-converting CatL-Like protease. Thus, two assays identified CatS as likely the major CatC-activating cysteine protease, whereas CatL could have a small contribution.

To determine whether the CatL and CatS proforms were processed by cysteine proteases, we resorted to the cell-permeable, broad-spectrum cysteine protease inhibitor, E64d (Fig. 4). Incubation of HL-60 cells with 100 μ M E64d for 72 h only delayed proCatS/proCatL processing, resulting in the appearance of low amounts of proCatL (Fig. 3C) and ~ 28-kDa-truncated proCatS (Fig. 3D). This indicated a partial involvement of at least one additional class of proteases. In this regard, CatD was identified in HL-60 cell lysates by both proteomic and immunoblot analyses. However, incubation of HL-60 cells with pepstatin A-penetratin conjugate (an inhibitor of acid proteases) did not alter the processing of proCatS and proCatL, thereby excluding CatD from the maturation pathways of these proteases (*data not shown*).

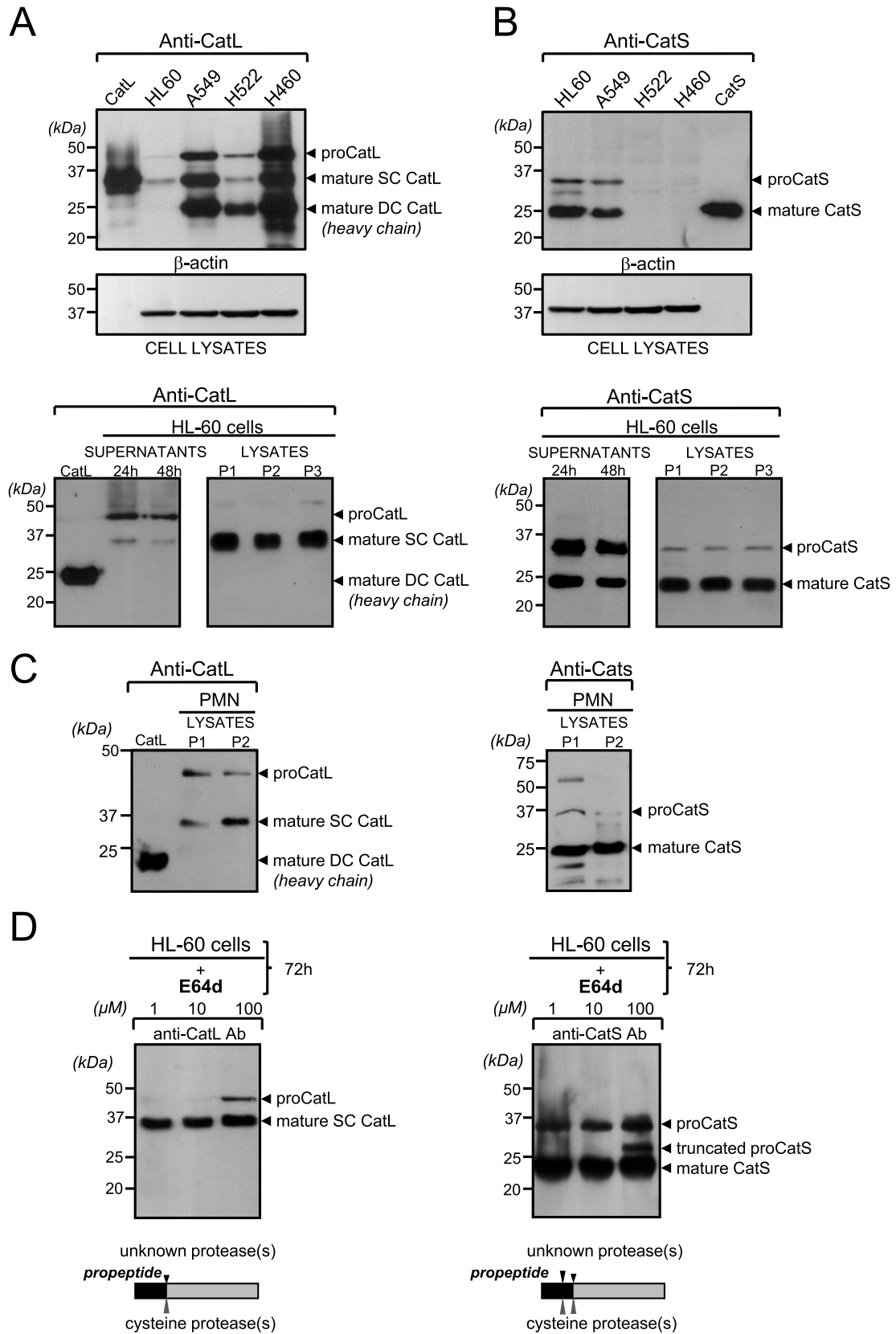
3.2. Impact of pharmacological CatS inhibition on the maturation of proCatC and proNSPs in human promyelocytic HL-60 precursor cells

In our previous study, we used IcatS to inhibit CatS [15] whereas in this study, we used two different CatS inhibitors expected to be more cell-permeable. A novel, potent, selective and cell-permeable CatS nitrile inhibitor, termed IcatS_{#54} (Fig. 4), was designed and synthesized, based on the IcatS [15]. IcatS_{#54} has improved cellular activity and selectively inhibits human CatS activity among other human cysteine cathepsins and NSPs (Tables 1 and 2). After incubating HL-60 cells with 10 μ M IcatS_{#54} for one week (i.e. the time required to allow a complete turnover of pre-existing active CatC and NSPs), we observed an important but still incomplete blockade of proCatC maturation, with accumulation of the previously reported 35-kDa fragment containing the truncated propeptide, the heavy chain and the light chain [21], and a low intensity band corresponding to the heavy chain (Fig. 5A). The proteolytic activity of CatC (monitored using its fluorogenic substrate, Gly-Phe-AMC) was inhibited ~ 95 % relative to control cell lysates. Despite this, the activity of PR3 and CatG were reduced by only 10–15 % (Fig. 5A). IcatS_{#54} also did not interfere with the processing of proCatS into the mature protease, as similar amounts of pro- and mature CatS were detected in treated and control cells by western blot. We confirmed the results using the potent, selective and cell-permeable CatS nitrile inhibitor, RO5461111 (Roche Pharma Research & Early Development, Roche Innovation Center Basel, hereafter called IcatS_{RO-11}, IC₅₀CatS = 0.4 nM; IC₅₀CatL = 49 μ M [44]) which blocked ~ 95 % of CatC activity in cell lysates resulting in the inhibition of PR3 and CatG by only 10–15 % (Fig. 5A). The presence of active PR3 and CatG in IcatS_{#54}-treated cell lysates was also confirmed by observing the formation of the ~ 80-kDa irreversible serpin-protease complexes when lysates were incubated with α 1PI (Fig. 5B). Similar results were obtained when IcatS_{RO-11}-treated cells were incubated with serpins (*data not shown*).

Although this is unlikely, the residual CatC activity (less than 5 %) observed in the presence of IcatS_{#54} or IcatS_{RO-11} may have been enough to fully activate proNSPs. To eliminate this possibility, we next tried to block proCatC maturation completely before measuring NSP activities.

3.3. Consequences of total proCatC maturation blockade on proNSPs in human promyelocytic HL-60 precursor cells

We used the cell-permeable aldehyde protease inhibitor, N-(4-fluorophenylsulfonyl)-L-valyl-L-leucinal (compound 1, 2S-[[[(4-fluorophenylsulfonyl)amino]-N-[(1S)-1-formyl-3-methylbutyl]-3-methylbutanamide [45]], to inhibit both CatS (IC₅₀ = < 1 nM) and CatL (IC₅₀ = 1.6 nM [45]) that did not reduce CatC/NSPs activities using purified proteases *in vitro*. Incubating HL-60 cells with compound 1 (10 μ M final), resulted in a nearly total abolition of proCatC maturation, with a



(caption on next page)

Fig. 3. CatL and CatS in HL-60 cells. Western blot analysis of 30-fold concentrated HL-60 cells supernatants (50 µg of protein/lane) and cell lysates (50 µg protein/lane) A) using antiCatL or B) antiCatS antibodies. The cells were cultured for 24 h and 48 h. Western blotting were performed in denaturing and reducing conditions using mature double chain purified human liver CatL [61], recombinant CatL and recombinant CatS as controls. Human lung cancer lines A549, H522, H460 expressing both mature single chain (SC) and double chains (DC) CatL were used for comparative analysis. Similar results were obtained in 3 independent experiments. C) Western blot analysis of human polymorphonuclear neutrophil (PMN) lysates using antiCatL or antiCatS antibodies. D) Processing of proCatL and proCatS in HL-60 cells exposed to increasing concentration of E64d. HL-60 cells were cultured in the presence of 1, 10 or 100 µM of E64d for 72 h and were lysed. Cell lysates were analyzed by western blotting in denaturing and reducing conditions using antiCatL or antiCatS antibodies. Two bands of ~ 42-kDa and ~ 28-kDa, corresponding, to proCatL and truncated proCatS, respectively, appeared when cells were incubated with 100 µM of E64d. Diagrams show the processing of proCatL and proCatS in HL-60 cells. Arrows indicate the cleavage sites in zymogens. As ~ 28-kDa truncated proCatS with comparable molecular weight was also observed during auto-processing [62,63], we assumed that the sequence cleavable by unknown protease(s) in proCatS propeptide segment was also cleaved by cysteine protease(s).

corresponding accumulation of the truncated proCatC fragment as observed by western blot (Fig. 6A). Accordingly, the proteolytic activity of CatC monitored with Gly-Phe-AMC in compound 1-treated versus control cells was inhibited by ~ 99 %. These effects could not be attributed to compound 1 toxicity, since preliminary experiments showed that it was non-toxic at up to 30 µM in HL-60 cells. Despite its marked inhibition of CatC activity, compound 1 failed to significantly affect PR3 or CatG activities (Fig. 6A). Compound 1 also did not affect the processing of proCatS, as similar amounts of pro- and mature forms were detected in treated and untreated cells by western blot (Fig. 6B). Similar results were obtained with two other aldehyde inhibitors of CatS/CatL, namely N-benzyloxycarbonyl-L-leucyl-norleucinal (IC₅₀CatS = 1.2 nM ±, IC₅₀CatL = 4 ± nM) and N-Acetyl-L-leucyl-L-leucyl-L-methioninal (IC₅₀CatS = 1.5 ± 0.88 nM, IC₅₀CatL = 3.2 ± 0.94 nM) or using cell-permeable dipeptidyl α-ketoamide reversible inhibitor Z-L-Abu-CONH-ethyl reported as compound 2, compound 3 and compound 4, respectively (Fig. 7). Because aldehyde protease inhibitors can also inhibit calcium-dependent cysteine proteases (calpains) within cells, we tested whether the maturation of proCatC might be affected by EGTA (a general calcium-dependent protease inhibitor), or by PD 150606 (3-(4-iodophenyl)-2-mercapto-(Z)-2-propenoic acid; a cell-permeable, non-competitive, selective, calcium-dependent inhibitor of calpain-1 and calpain-2). Neither inhibitor altered the maturation of proCatC, indicating no implication of calpain-type proteases in this process (*data not shown*).

These data from indirect CatC inhibition studies suggested that at least one additional protease that was not able to hydrolyse the Gly-Phe-AMC CatC substrate, was involved in CatS/CatC-independent maturation of proPR3/proCatG in HL-60 cells. This CatC-like protease(s), now called NSPs-Alternative Activating Protease-1 (NSPs-AAP-1), was capable of activating 80 % of PR3 and CatG when proCatC maturation was almost totally inhibited. We then investigated whether we could inhibit NSPs-AAP-1 using chemical inhibitors targeting CatC, by analyzing NSP activation in HL-60 cells.

3.4. Co-inhibition of both CatC and NSPs-AAP-1 in human promyelocytic HL-60 precursor cells by reversible nitrile CatC inhibitor IcatC_{XPZ-01}

Since IcatC_{XPZ-01}, a potent, reversible, cell-permeable nitrile inhibitor [25] inhibits ~ 95 % of CatC activity in HL-60 cells but in contrast to IcatS_{#54}, almost completely prevented proNSPs maturation [15], we hypothesized that IcatC_{XPZ-01} must inhibit not only CatC, but also NSPs-AAP-1. Indeed, supplementing compound 1 with IcatC_{XPZ-01} at days 7 and 10 resulted in ~ 95 % inhibition of PR3 and CatG in cell lysates (Fig. 6A). Furthermore, we observed that the combination of both compound 1 and IcatC_{XPZ-01}, but not the individual inhibitors, partially altered proCatS maturation with appearance of the ~ 28-kDa-truncated proCatS (Fig. 6B). Furthermore, when compound 1 was supplemented with IcatC_{XPZ-01}, we detected unprocessed, proteolytically inactive PR3 zymogens that were unable to form an irreversible stable complex with α1PI (Fig. 6C).

Thus, NSPs-AAP-1 that, together with CatC, is involved in proPR3/proCatG maturation was inhibited by IcatC_{XPZ-01} (Fig. 6D). We then analyzed the NSPs-AAP-1 dependent activation of proNSPs using additional CatC inhibitors.

3.5. Inhibition of CatC-, but not NSPs-AAP-1-dependent activation of proNSPs, by irreversible CatC inhibitors in human HL-60 cells

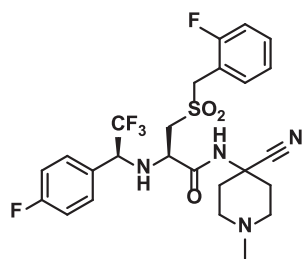
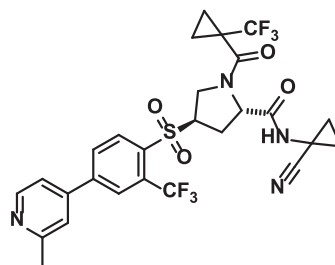
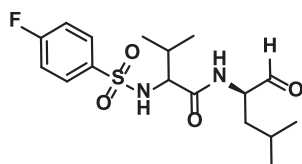
We hypothesized that irreversible CatC inhibitors GSK-2793660 (IcatC_{GSK-60}) [31] and EGFR-derived inhibitor (IcatC_{EGFR-22}) [32], which are structurally distinct from IcatC_{XPZ-01}, inhibit CatC but not the NSPs-AAP-1 pathway. Incubation of HL-60 cells with IcatC_{GSK-60} (10 µM) or IcatC_{EGFR-22} (0.2 µM) for one week resulted in an almost total abolition of the cleavage of Gly-Phe-AMC substrate, indicating effective CatC inhibition (IcatC_{EGFR-22}: 99.9 ± 0.14 %; IcatC_{GSK-60}: 98 ± 0.53 %; n = 3 independent experiments). However, cell treatment with IcatC_{GSK-60} or IcatC_{EGFR-22} reduced the PR3/CatG activity by only 10–20 %. Therefore, NSPs-AAP-1 contributed to ~ 85 % of PR3 and CatG activation when CatC was almost totally inhibited. Similar results were found when IcatC_{GSK-60} was supplemented with compound 1. Unlike IcatC_{XPZ-01}, the combination of IcatC_{GSK-60} with compound 1 did not alter proCatS maturation (western blot analysis, n = 3 independent experiments).

These results showed that IcatC_{GSK-60} and IcatC_{EGFR-22} inhibited CatC but not the NSPs-AAP-1 activity and confirmed that the latter represents an additional protease involved in the maturation of proNSPs in HL-60 cells. We next investigated consequences of CatC zymogen maturation blockade on NSP maturation in neutrophils generated from human CD34⁺ progenitor cells.

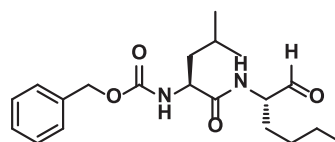
3.6. Consequences of proCatC maturation blockade on proNSP activation in neutrophils generated from human CD34⁺ progenitor cells

Human CD34⁺ HSC were isolated from umbilical cord blood and differentiated into neutrophils in the presence or absence of CatS inhibitor IcatS_{#54} (20 µM) (Fig. 8A). Neutrophil differentiation was assessed by the expression of neutrophil surface markers (CD11b, CD15, CD66b) but was not affected by the inhibitory compounds after 10 days (*data not shown*). By western blot, we observed nearly no proCatC maturation as evidenced by minimal accumulation of the 35-kDa truncated proCatC fragment in IcatS_{#54}-treated cells (Fig. 8B). Immunoblotting of cell lysates showed no alteration of MPO processing as a control but reduction of the amount of NSP zymogens (Fig. 8C, D). NSP activities in IcatS_{#54}-treated cell lysates were significantly but incompletely inhibited (by 62.5 ± 11.7 % for PR3, by 76.4 ± 14.7 % for NE and by 62.4 ± 8.1 % for CatG) as determined by hydrolysis of the sensitive and selective FRET substrates (n = 3 independent experiments) (Fig. 8E). Importantly, combination of IcatS_{#54} with IcatC_{XPZ-01} resulted in almost total inhibition and elimination of NSPs (Fig. 8D and E) without affecting cell differentiation. A similar partial NSPs inhibition was obtained when human CD34⁺ HSC were differentiated in the presence of compound 1. Again, when compound 1 was combined with the nitrile CatC inhibitor, IcatC_{BI-9740}, NSP activities were abrogated (Fig. 9).

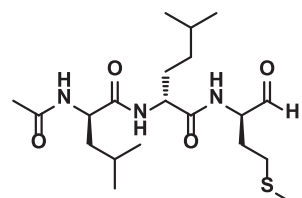
In conclusion, we identified CatS as the major human neutrophil proCatC maturing protease involved in proNSP activation, and NSPs-AAP-1 as an additional CatC-independent protease that activates proNSPs and was inhibited by reversible nitrile inhibitors. We next investigated proteolytic pathways involved in the activation of NSPs in mice.

IcatS_{#54}IcatS_{RO-11}

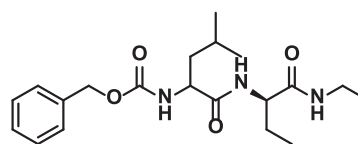
Compound 1



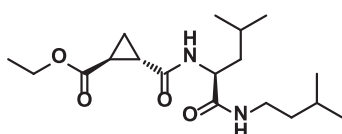
Compound 2



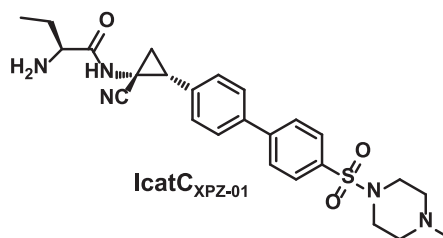
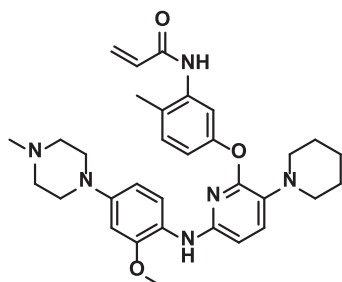
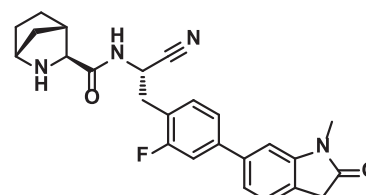
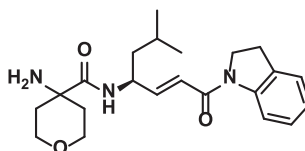
Compound 3



Compound 4



E64d

IcatC_{XPZ-01}IcatC_{EGFR-22}IcatC_{BI-9740}IcatC_{GSK-60}

(caption on next page)

Fig. 4. Chemical structures of cell-permeable synthetic protease inhibitors used in this study. **IcatS_{#54}**: (R)-N-(4-cyano-1-methylpiperidin-4-yl)-3-((2-fluorobenzyl)sulfonyl)-2-(((S)-2,2,2-trifluoro-1-(4-fluorophenyl)ethyl)amino)propenamide, **RO5461111 (IcatS_{RO-11})**: (2S,4R)-N-(1-cyanocyclopropyl)-4-((4-(2-methylpyridin-4-yl)-2-(trifluoromethyl)phenyl)sulfonyl)-1-(1-(trifluoromethyl)cyclopropane-carbonyl)pyrrolidine-2-carboxamide (*CatS* inhibitors), **Compound 1**: 2S-[[[(4-fluorophenyl)sulfonyl]amino]-N-[(1S)-1-formyl-3-methylbutyl]-3-methyl-butanamide, **Compound 2**: (calpeptin, *N*-benzyloxycarbonyl-L-leucyl-norleucinal); **Compound 3**: (N-Acetyl-L-leucyl-L-leucyl-L-methioninal, **Compound 4**: (Z)-L-Abu-CONH-ethyl) (*CatS* and *CatL* inhibitors), **E64d**: (1S,2S)-ethyl 2-(((S)-1-(isopentylamino)-4-methyl-1-oxopentan-2-yl)carbamoyl)cyclopropanecarboxylate (*broad-spectrum cysteine protease inhibitor*), **IcatC_{XPZ-01}**: (S)-2-amino-N-((1R,2R)-1-cyano-2-(4-(4-methylpiperazin-1-yl)sulfonyl)biphenyl-4-yl)cyclopropyl)butanamide, **Compound 22 (IcatC_{EGFR-22})**: N-(5-(((2-methoxy-4-(4-methylpiperazin-1-yl)phenyl)amino)-3-(piperidin-1-yl)pyridin-2-yl)oxy)-2-methylphenyl)acrylamide, **BI-9740 (IcatC_{BI-9740})**: (1R,3S,4S)-N-((S)-1-cyano-2-(2-fluoro-4-(1-methyl-2-oxoindolin-6-yl)phenyl)ethyl)-2-azabicyclo[2.2.1]heptane-3-carboxamide, **GSK2793660 (IcatC_{GSK-60})**: (S,E)-4-amino-N-(1-(indolin-1-yl)-6-methyl-1-oxohept-2-en-4-yl)tetrahydro-2H-pyran-4-carboxamide (*CatC* inhibitors).

Table 1

Comparative analysis of **IcatS_{#54}** selectivity for human cysteine cathepsins and NSPs.

Proteases	IC ₅₀ (nM)
CatS	7.1
CatB	>10.000
CatC	n.i.
CatK	>10.000
CatL	358
CatV	139
NE	n.i.
PR3	n.i.
CatG	n.i.

IC₅₀ concentration of **IcatS_{#54}** resulting in 50% inhibition of proteolytic activity.

n.i.: non inhibition

Table 2

Proteases targeted with cell-permeable synthetic inhibitors used in this study.

Inhibitors	Targeted proteases
• <i>Reversible covalent</i>	
IcatS_{#54}	CatS
IcatS_{RO-11}	CatS
Compounds 1–4	CatS and CatL
IcatC_{XPZ-01}	CatC and NSPs-AAP-1
IcatC_{BI-9740}	CatC and NSPs-AAP-1
• <i>Irreversible</i>	
IcatC_{EGFR-22}	CatC
IcatC_{GSK-60}	CatC
E64d	Cysteine proteases

3.7. Consequences of *CatS* genetic depletion on proCatC and proNSP maturation in mice

We investigated whether proCatC/proNSPs were processed and matured in C57BL/6 *CatS* knock-out (*Ctss*^{-/-}) mice. Western blots using bone marrow and blood WBC lysates from *Ctss*^{-/-} animals showed that proCatC was correctly processed and that amounts of the heavy chains liberated were the same in WT and *Ctss*^{-/-} lysates (Fig. 10A and B). These finding did not eliminate the possibility of temporary *CatS* involvement, namely in proCatC maturation in promyelocytes, affecting proNSPs conversion into active enzymes. NE was detected in the bone marrow and in blood WBC lysates, and formed irreversible 80-kDa complexes when lysates were incubated with exogenous purified α 1PI, as determined by western blot (Fig. 10C). The selectivity of anti-murine NE antibodies was shown in bone marrow-derived WBC or isolated bone marrow neutrophils from NSP triple knock-out mice (*data not shown*). These data suggest that *CatS* was not the major proCatC maturing protease in mice and not a major contributor to NSPs activation.

3.8. Consequences of *CatC* genetic depletion or pharmacological inhibition on proNSP activation in mice

We next investigated the presence of NSPs-AAP-1 in mice. Bone

marrow samples were collected from WT and *Ctsc*^{-/-} C57BL/6 mice and *CatC*/*NSPs* were analyzed in cell lysates by immunoblot and fluorogenic substrate assay (Fig. 11). The selectivity of murine NSP substrates and antibodies was checked in bone marrow-derived WBC or isolated neutrophils from NSP triple knock-out mice ($n \geq 3$ independent experiments (*data not shown*)). Western blots using selective antibodies showed significantly reduced but still detectable NSP proteins (30.7 % \pm 2.8 for NE and 20.2 % \pm 1.7 for CatG) in samples from *Ctsc*^{-/-} mice (Fig. 11A, middle and lower panels). Moreover, NSPs detected in bone marrow lysates from *Ctsc*^{-/-} mice formed irreversible 80-kDa complexes when lysates were incubated with exogenous purified α 1PI or ACT, as determined by western blotting (*data not shown*). Accordingly, significantly reduced but still substantial NSP activities were measured (36.34 % \pm 8.62 for NE, 46.2 % \pm 6.29 for PR3 and < 1 % for CatG (Fig. 11B)) in bone marrow samples from *Ctsc*^{-/-} mice compared to WT mice. Residual NE and PR3 activities were more pronounced than that of CatG. Residual NSP activities were inhibited in the presence of selective NSP inhibitors (*data not shown*). Collectively, these results showed that *CatC* was also the unique protease involved in proNSP maturation in mice, and that an NSPs-AAP-1 was also present in mice and a contributor to NSP activity (Fig. 11C).

We then studied the inhibition of murine NSPs-AAP-1 in the presence of *CatC* inhibitor **IcatC_{XPZ-01}** *in vitro* and *in vivo*. In these experiments, WT or *Ctsc*^{-/-} murine neutrophils were differentiated from bone marrow progenitors *in vitro* in WT. Detectable NSP activities were measured in differentiated *Ctsc*^{-/-} neutrophils (NE: 18.0 \pm 5.4 %; PR3: 20.0 \pm 6.6 %; CatG 0.1 \pm 0.1 %, relative to neutrophils from WT animals) (Fig. 12A) but not in NSP triple knock-out bone marrow isolated mature neutrophils used as controls ($n \geq 3$ independent experiments). Moreover, we observed an almost total inhibition of NSP proteolytic activities when WT and *Ctsc*^{-/-} neutrophils were differentiated in the presence of 1 μ M of **IcatC_{XPZ-01}** that inhibits both *CatC* and NSPs-AAP-1 in 5 independent experiments (Fig. 12A). Prolonged administration (7 days) of **IcatC_{XPZ-01}** (4.8 mg/kg at 10 ml/kg as in [25]) treatment reduced NSP proteolytic activities (by 29.1 \pm 8.3 % for NE, 20.4 \pm 5.7 % for PR3 and 26.3 \pm 9 % for CatG) (Fig. 12B) and NSP proteins (by 81.1 \pm 6.8 % for NE and 75.9 \pm 8.6 % for CatG) (Fig. 12C) in WT mice as assessed at the end of the treatment period.

4. Discussion

In this study, we show (i) that *CatS*, a potent elastolytic enzyme, is the major druggable converting protease involved in the maturation of human neutrophil proCatC; (ii) that an NSPs-AAP-1 activity exists and works independently of *CatC* in granulocytes; (iii) that proNSPs are activated by *CatC*- and NSPs-AAP-1-dependent proteolytic pathways, which are conserved in both humans and mice; and (iv) that pharmacological targeting of *CatS* in human CD34⁺ hematopoietic stem cell-differentiated neutrophils allows for a sizeable inactivation and elimination of NSPs (~70 %), as well as a further reduction upon additional NSPs-AAP-1 inhibition. These heretofore unknown aspects of the proteolytic pathways involved in proNSP activation have the potential to spawn novel treatment strategies to control NSP-mediated tissue injury that is often associated with the presence of activated neutrophils in numerous chronic inflammatory or autoimmune diseases.

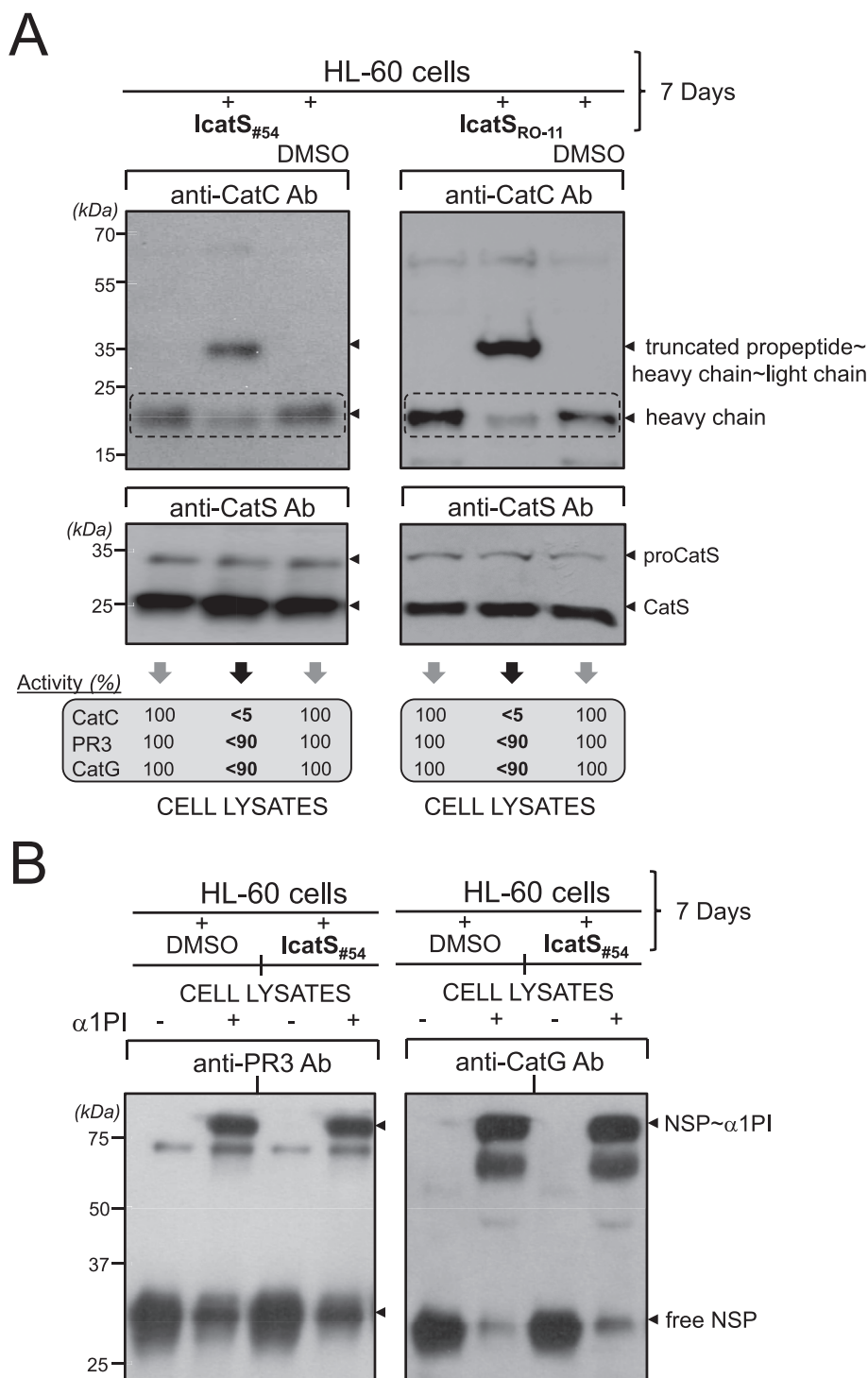


Fig. 5. Consequences of pharmacological CatS inhibition on the maturation of proCatC and proNSPs in HL-60 cells. HL-60 cells were cultured for 7 days in the presence of 10 μM of IcatS_{RO-11} or IcatS_{#54} or after adding DMSO containing medium alone. A) Western blot analysis of cell lysates using antiCatC antibody directed against the 23-kDa heavy chain of CatC demonstrating the accumulation of ~ 35-kDa fragment composed of truncated propeptide, the heavy chain and the light chain in presence of IcatS_{RO-11} or IcatS_{#54}. Western blot analysis of cell lysates using antiCatS antibody as protein control showing not impact of inhibitors on proCatS processing. The percentage of proteolytic activities of CatC, PR3 and CatG was determined using fluorogenic substrates GF-AMC, Abz-VAD(nor)VADYQ-EDDnp, and Abz-TPFSGQ-EDDnp, respectively. Similar results were obtained in three independent experiments. B) Western blot analysis of cell lysates incubated with or without human α1PI using antiPR3 or antiCatG antibody. The *de novo* formation of irreversible α1PI-NSP complexes of about 75-kDa revealing activation of PR3 and CatG in presence of IcatS_{#54}.

CatL and CatS have been previously identified as proCatC-maturing proteases *in vitro* [14]. We have similarly investigated the maturation of proCatC in human neutrophilic precursors at different stages and showed that targeting CatS using a selective cell-permeable

nitrile inhibitor (IcatS) reduced CatC activity by about 80 % without affecting NSP activities [15]. We had proposed that this incomplete CatC inhibition could be due to the presence of additional proCatC maturing protease(s) resistant to the CatS inhibitor and/or to a limited effect of the

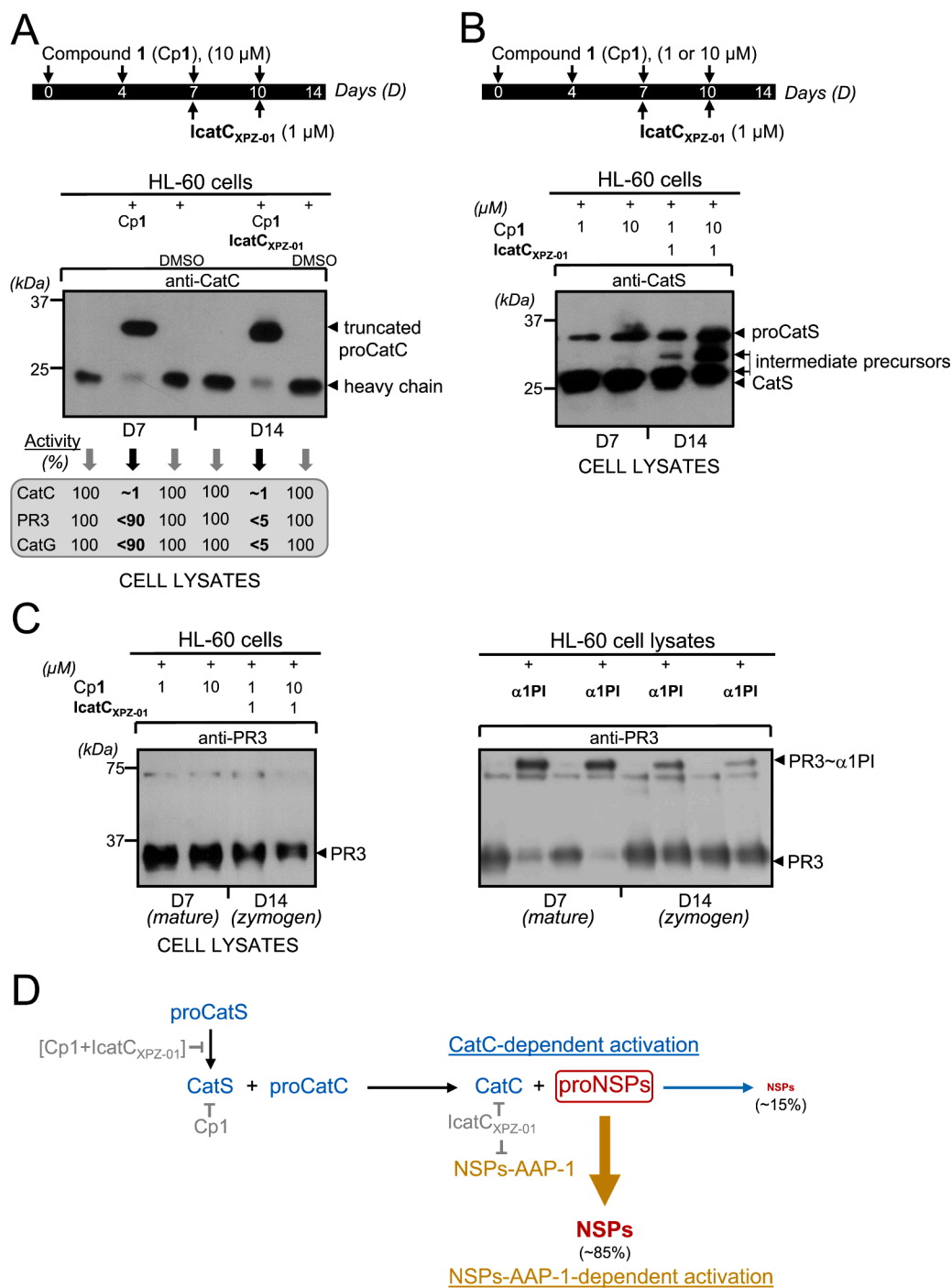


Fig. 6. Processing of proCatC, proCatS and proNSPs in HL-60 cells cultured in the presence of compound 1 supplemented with IcatC_{XPZ-01}. HL-60 cells were cultured for 14 days in the presence of compound 1 or after adding DMSO containing buffer alone. IcatC_{XPZ-01} was added at day 7. Processing of proCatC, proCatS and proNSPs in cell lysates were analyzed by western blotting. A) Western blot analysis of cell lysates using anti-CatC antibody directed against the 23-kDa heavy chain of CatC demonstrating the accumulation of ~ 35-kDa fragment in presence of compound 1. Proteolytic activities of NSPs are inhibited in presence of compound 1 supplemented with IcatC_{XPZ-01}. The percentage of proteolytic activities of CatC, PR3 and CatG was determined as in Fig. 5. Results obtained in three independent experiments were shown. B) Western blot analysis of cell lysates using anti-CatS antibody showing alteration of proCatS processing with accumulation of intermediate precursor in presence of compound 1 supplemented with IcatC_{XPZ-01}. Similar results were obtained in three independent experiments. Incubation of cells only with compound 1 (*data not shown*) or IcatC_{XPZ-01} for 14 days did not alter the processing of proCatS (see Fig. 7C). C) Western blot analysis of cell lysates incubated with or without α 1PI using anti-PR3 antibody. (*Left*) PR3 stability in cell lysates incubated without α 1PI. (*Right*) PR3 in same cell lysates incubated with or without α 1PI. The decrease of ~ 75-kDa irreversible α 1PI-PR3 complexes formation and the detection of free PR3 in presence of compound 1 supplemented with IcatC_{XPZ-01} revealing unprocessing of PR3 zymogens. Similar results were obtained in three independent experiments. D) Diagram summary of proNSPs activation pathways in HL-60 cells. ProNSPs are activated by CatC (*in blue*) and NSPs-AAP-1 (*in dark yellow*) dependent pathways in HL-60 cells. CatC dependent activation pathway is initiated by proteolytic processing and maturation of proCatS. Combination of compound 1 with IcatC_{XPZ-01} partially inhibits the maturation of proCatS. The nitrile dipeptidyl CatC inhibitor IcatC_{XPZ-01} inhibits both CatC and NSPs-AAP-1 dependent maturation of proNSPs in HL-60 cells.

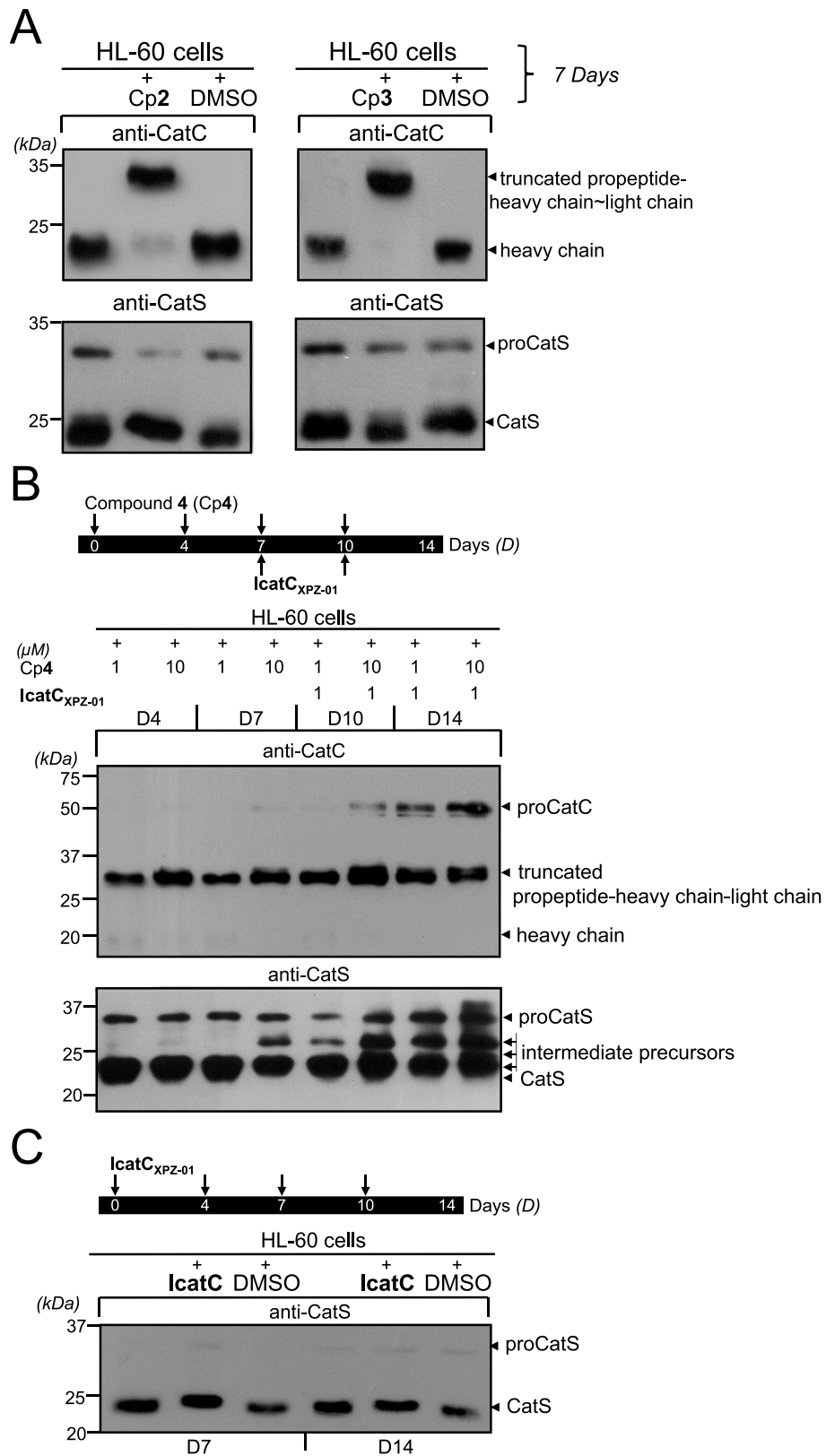


Fig. 7. Processing of proCatC and proCatS in HL-60 cells cultured in the presence or absence of synthetic inhibitors. **A)** HL-60 cells were cultured for 7 days in the presence of compound 2 (Cp2, 10 μM), compound 3 (Cp3, 10 μM) or after adding DMSO containing buffer alone. Cell lysates were analyzed by western blotting using antiCatC antibody. **B)** HL-60 cells were cultured for 14 days in the presence of compound 4 (Cp4, 1 and 10 μM), or after adding buffer containing DMSO alone. **IcatC_{XPZ-01}** (1 μM) was added at days 7 and 10. Cell lysates were analyzed by western blotting using antiCatC antibody and antiCatS antibody. **C)** HL-60 cells were cultured for 14 days in the presence of **IcatC_{XPZ-01}** (1 μM), or after adding buffer containing DMSO alone. Cell lysates were analyzed by western blotting using antiCatS antibody.

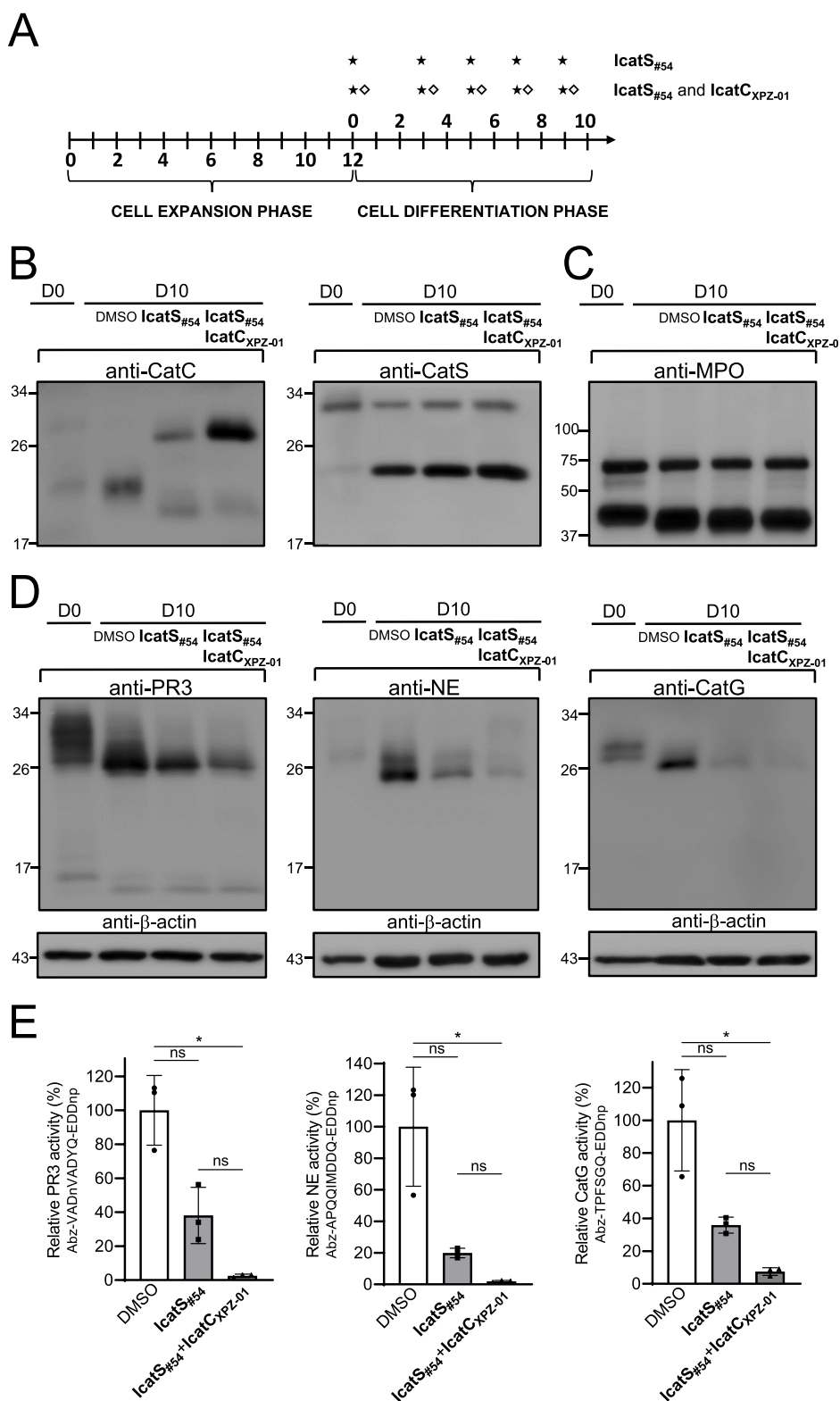
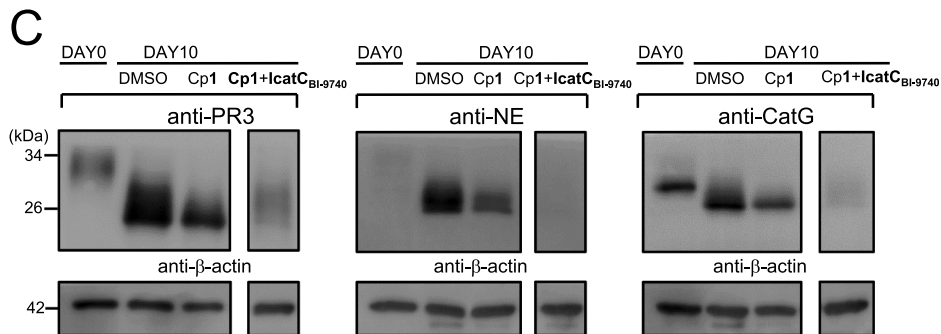
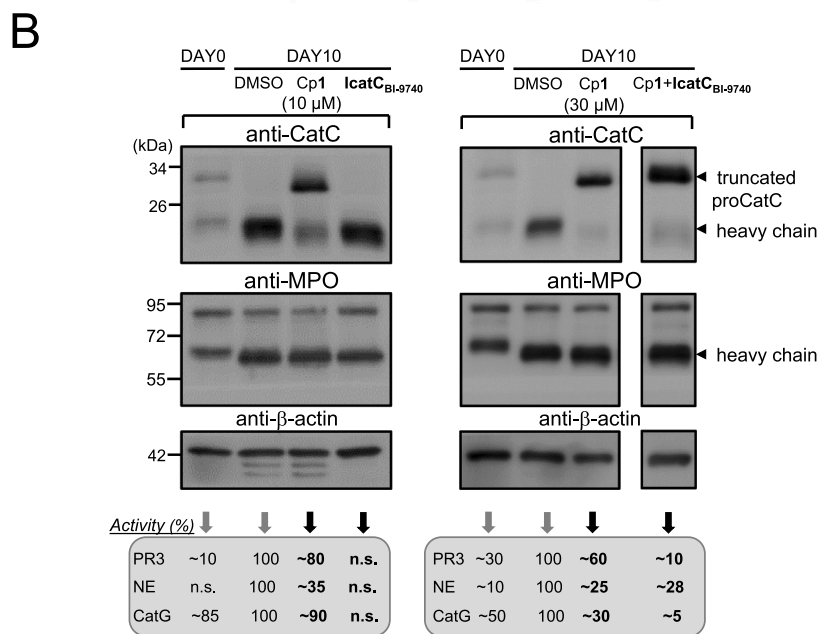
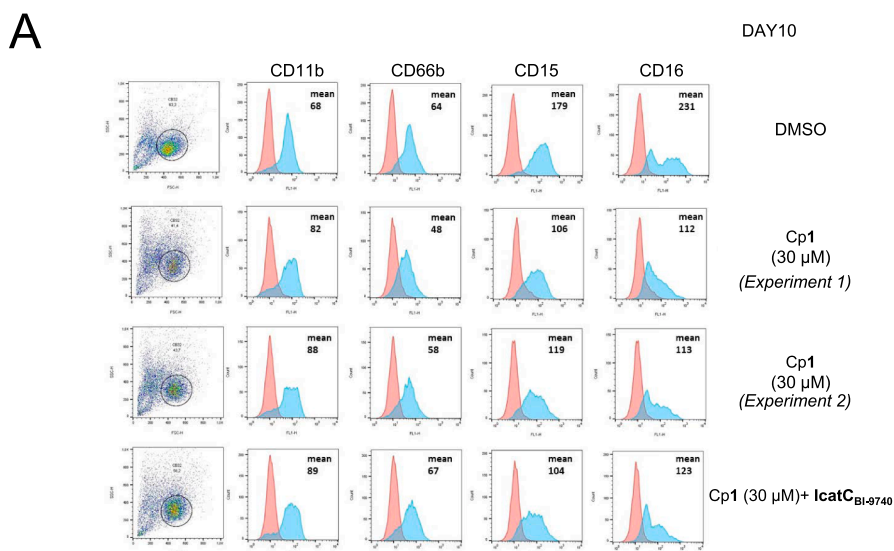


Fig. 8. Activation of proNSPs in neutrophils generated from CD34⁺ hematopoietic stem cells in the presence of IcatS_{#54}. A) CD34⁺ cells from umbilical cord blood samples of three donors were differentiated over 10 days into neutrophils in medium containing IcatS_{#54} (20 μM), a mixture of IcatS_{#54} (20 μM) and IcatC_{XPZ-01} (1 μM), or in DMSO containing buffer, respectively. B) Immune reactive CatC and CatS. C) MPO as a control was not affected by inhibitor treatment. D) PR3, NE and CatG were analyzed in cell lysates in parallel by western blotting using specific antibodies. Anti-β-actin was used as loading control. Western blot analysis of cell lysates demonstrating the elimination of NSP zymogens in presence of inhibitors. E) Proteolytic activity for PR3, NE, and CatG was determined by FRET assay. Proteolytic activity was strongly reduced in the presence of the CatS (IcatS_{#54}) inhibitor alone and almost abrogated by the combination with the CatC inhibitor (IcatC_{XPZ-01}). Statistical analysis of the data was performed using a nonparametric test (Kruskal-Wallis test), *p < 0.1.



(caption on next page)

Fig. 9. Activation of proNSPs in neutrophils generated from CD34⁺ hematopoietic stem cells in the presence of compound **1** alone and in combination with the reversible nitrile CatC inhibitor **IcatC_{BI-9740}**. CD34⁺ cells from umbilical cord blood samples of three donors were differentiated over 10 days into neutrophils in medium containing compound **1** (Cp1, 10 μ M or 30 μ M), **IcatC_{BI-9740}** (1 μ M), compound **1**/**IcatC_{BI-9740}** or after adding DMSO containing buffer alone. A) Neutrophil differentiation was assessed by the expression of the neutrophil surface markers CD11b, CD66b, CD15 and CD16 (blue) by flow cytometry. Isotype staining in (red). B) Processing of proCatC in cell lysates were analyzed by Western blotting using antiCatC antibody directed against the 23-kDa heavy chain of CatC. Western blot analysis of cell lysates demonstrating the accumulation of the fragment composed of truncated propeptide, the heavy chain and the light chain in presence of compound **1** (10 μ M, two independent experiments; 30 μ M, one experiment). Anti-myeloperoxidase (MPO) and anti- β -actin used as controls. NSPs activities were determined in the same cell lysates prepared for CatC analysis as in Fig. 8. Incubation of cells with **IcatC_{BI-9740}** alone resulted in complete elimination of NSPs in cell lysates as in [26] (*data not shown*). C) Immune reactive PR3, NE and CatG were analyzed by Western blotting using antiPR3, antiNE and antiCatG antibodies in the same cell lysates prepared for CatC analysis as in Fig. 8. Anti- β -actin used as loading control. Western blot analysis of cell lysates demonstrating the reduction of NSP zymogens in presence of compound **1** alone (30 μ M) and complete inhibition in combination with **IcatC_{BI-9740}**.

inhibitor in the cell-based assay. In this study, we aimed to block completely the maturation of proCatC using synthetic, cell-permeable cysteine cathepsin inhibitors and to determine the fate of NSPs in human neutrophilic precursors. Though we recently identified CatL-like proteases (CatF, CatK, CatV) as novel putative proCatC activators *in vitro* [21], herein we failed to detect these proteases in HL-60 cell lysates or supernatants. This agrees well with previous studies showing that the CatF gene is not expressed in HL-60 cells or leukocytes [46] while those of CatK and CatV are expressed mainly in osteoclasts [47,48] and in the thymus and testis [49]. CatS (and to a lower extent, CatL) were detected in both HL-60 cells and purified blood neutrophils, emerging as likely candidates to activate proCatC. CatL was detected as a ~ 32-kDa mature single chain (i.e. not processed into two mature 23-kDa chains) in HL-60

cells, much like it is found in fibroblasts [50] and bone marrow dendritic cells [51]. The wide-spectrum cysteine protease inhibitor, **E64d**, only partially altered proCatS and proCatL processing in HL-60 cells, indicating that activation of these two proteases obeys a non-specific proteolytic mechanism.

When we incubated HL-60 cells with **IcatS_{#54}**, the processing and maturation of proCatC were strongly altered and corresponded with the accumulation of a truncated proCatC fragment. This confirmed the prominent role of CatS, and fully agrees with data obtained using another nitrile inhibitor, **IcatS_{RO-11}**, which is structurally unrelated to **IcatS_{#54}** [44,52]. Noteworthy is that a residual CatC activity of about 5 % (vs that of control cells) was still present despite the complete inhibition of CatS by either **IcatS_{#54}** or **IcatS_{RO-11}**. More importantly, PR3

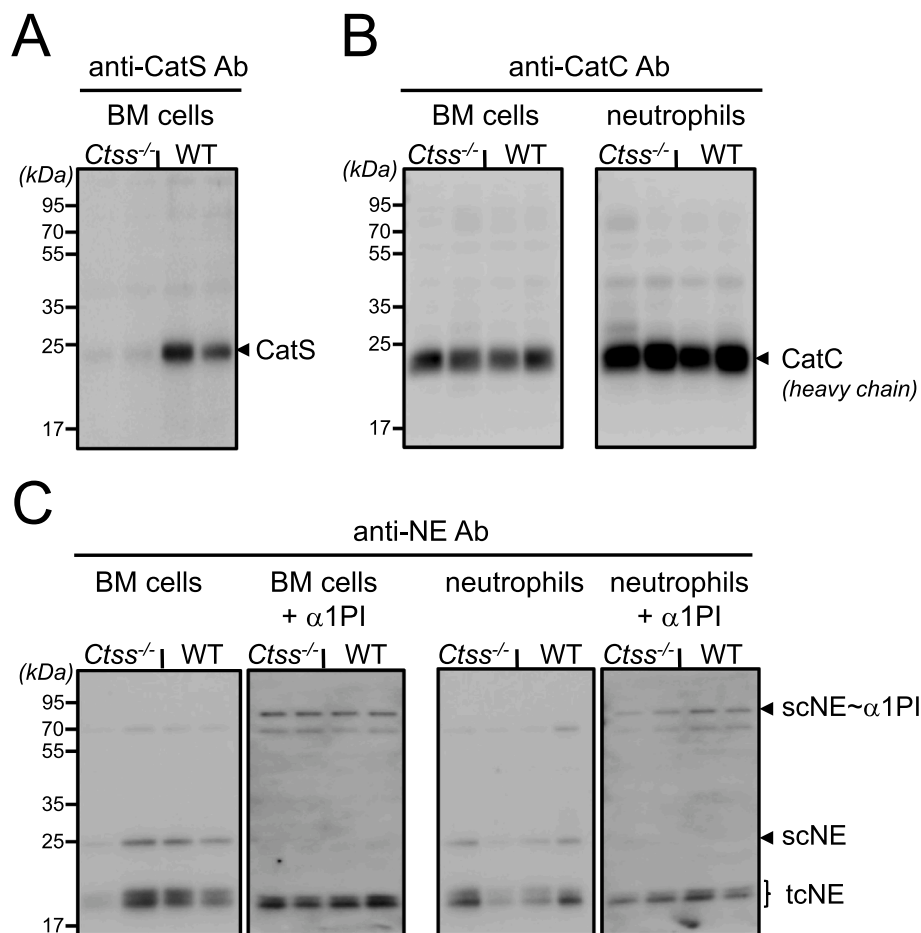


Fig. 10. Activation of CatC and NSPs in *Ctss*^{-/-} C57BL/6 mice. A) Western blot analysis of WT and *Ctss*^{-/-} bone marrow (BM) cell lysates using anti-CatS antibodies. B) Western blot analysis of bone marrow cells and blood neutrophils lysates using anti-CatC antibodies. Presence of mature immunoreactive CatC as revealed by the ~ 20-kDa heavy chain in *Ctss*^{-/-} mice indicates that CatS is not required in proCatC maturation. C) Western blot analysis of bone marrow cells and blood neutrophils lysates incubated with or without human α 1PI using anti-NE antibodies. The *de novo* formation of irreversible α 1PI-scNE complexes of about 80-kDa reveals that NE is proteolytically active despite the absence of CatS. NE produced by murine neutrophils may be present in a cleaved (two-chains (tc)) and uncleaved (single chain (sc)) [64]. Similar results were obtained in three independent experiments.

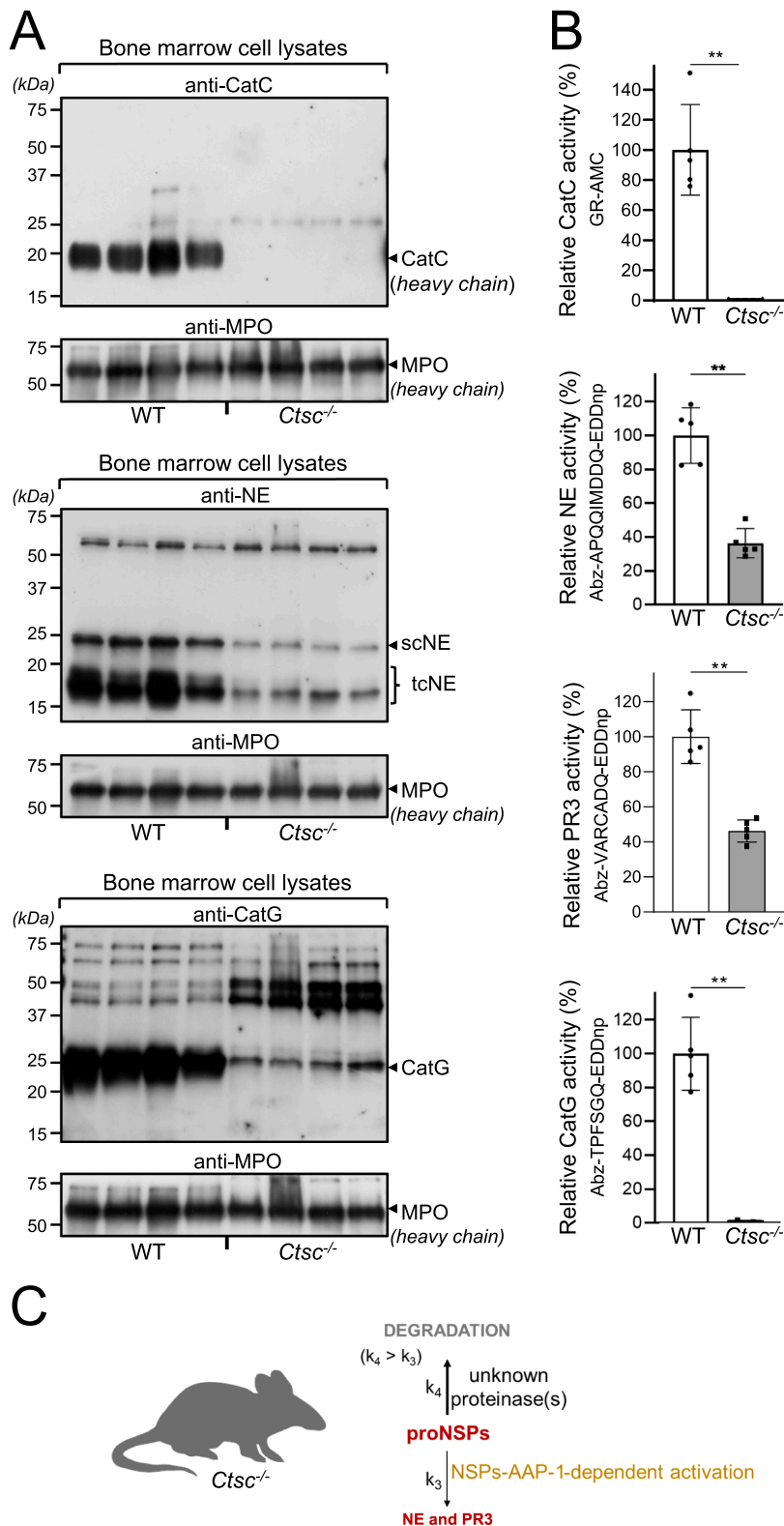
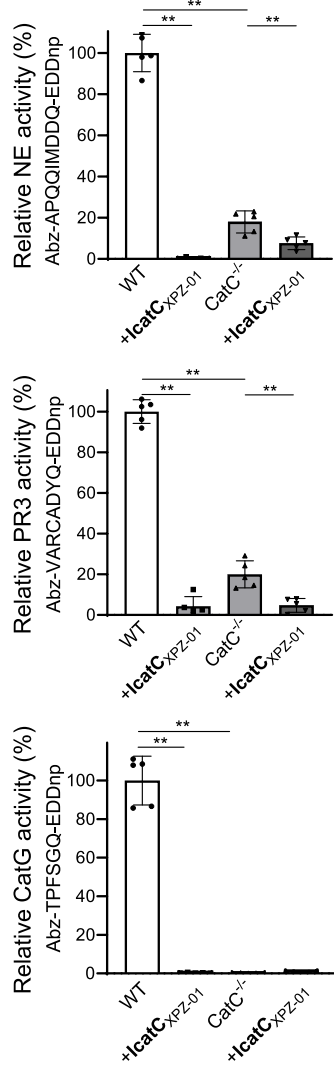
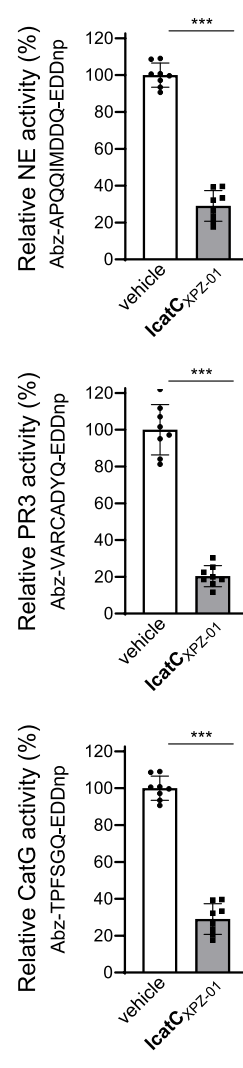


Fig. 11. Activation of NSPs in *Ctsc*^{-/-} C57BL/6 mice. A) Western blot analysis of bone marrow cell lysates using antiCatC, antiNE and antiCatG antibodies. Significantly reduced level of immunoreactive NE and CatG in *Ctsc*^{-/-} mice bone marrow lysates compared with WT shows the elimination of NSP zymogens in absence of CatC (n = 4 animals). sc: single chain/tc: two chains (upper and lower bands). Myeloperoxidase (MPO) served as control for protein content. B) Residual activity of CatC, NE, PR3 and CatG in *Ctsc*^{-/-} mice bone marrow lysates. Proteolytic activities were measured using fluorogenic substrates. Monitored selective NE, PR3 and CatG activities indicates the activation of NSPs in absence of CatC. The histograms show the mean ± SD of CatC (n = 5 animals) and NSP activities (n = 5 animals), each done in duplicates. Statistical analysis of the data was performed using a nonparametric test (Mann Whitney test), **p < 0.01. C) Consequences of CatC depletion in *Ctsc*^{-/-} mice on the fate of proNSPs. Activation and degradation pathways of proNSPs identified in PLS patients are conserved in CatC deficient mice.

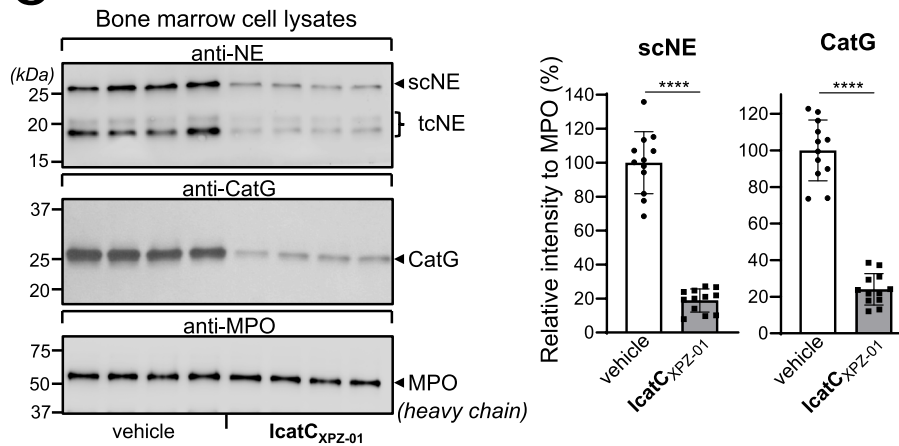
A



B



C



(caption on next page)

Fig. 12. Murine NSPs activation in presence of **IcatC_{XPZ-01}** in cellular assay *in vitro* and *in vivo*. A) Residual activity of NSPs in murine neutrophils differentiated from WT or *Ctsc*^{-/-} mice bone marrow progenitors in the presence of **IcatC_{XPZ-01}** *in vitro*. Almost total inhibition of NSP proteolytic activities measured using selective FRET substrates were observed. The histograms show the mean \pm SD in 5 independent experiments each done in duplicates. Statistical analysis of the data was performed using a nonparametric test (Mann Whitney test), ***p* < 0.01. B) Consequences of prolonged **IcatC_{XPZ-01}** administration into WT mice on NSPs activation. Residual activity of NSPs in bone marrow cell lysates were measured as in A. The histograms show the mean \pm SD in 5 independent experiments each done in duplicates. Statistical analysis of the data was performed using a nonparametric test (Mann Whitney test), ***p* < 0.01, ****p* < 0.001. C) Western blot analysis of bone marrow cell lysates using antiNE and antiCatG antibodies. Significantly reduced level of immunoreactive NE and CatG in **IcatC_{XPZ-01}** treated mice bone marrow lysates compared with vehicle treated control mice shows the elimination of NSP zymogens (n = 4 animals). Band intensities were normalized to myeloperoxidase (MPO) as loading control. The histograms show the mean \pm SD of 12 independent experiments. Statistical analysis of the data was performed using a nonparametric test (Mann Whitney test), *****p* < 0.0001. sc: single chain/tc: two chains (upper and lower bands).

and CatG (chosen here as representative NSPs) remained fully active.

This raises the question of whether the residual CatC activity observed when CatS is inhibited is sufficient to fully activate NSPs, or whether other protease(s) might compensate for the low level of CatC activity. In this regard, **IcatS_{#54}** is a reversible inhibitor that could well spare a low level of active CatS, hardly detectable kinetically but sufficient to explain the partial CatC activation. It could also be that CatL, which is present in low amounts in HL-60 cells and is not inhibited by **IcatS_{#54}**, is responsible for this activation. We succeeded in fully blocking proCatC maturation using cell-permeable cysteine protease inhibitors that target both CatS and CatL (compounds 1–4). However, we found again that PR3 and CatG remained almost fully active. Thus, HL-60 cells contain at least one additional protease that can activate proPR3 and proCatG. We and others observed that in neutrophils from PLS patients who totally lack CatC, strongly reduced but still detectable active PR3/NE (0.5 % to 10 % versus healthy controls), and active CatG (<1% versus healthy controls) [19,22] were present. These data strongly suggest the existence of an unknown alternative protease(s) involved in proNSP activation. A CatC-like protease with such a profile, which we termed NSPs-AAP-1, is a cysteine protease inhibited by reversible nitrile inhibitors of CatC, but not by irreversible ones. Interestingly, this proteolytic activity is inhibited by **IcatC_{XPZ-01}** since we observed no

significant activation of proPR3 or proCatG when supplementing compounds 1–4 with **IcatC_{XPZ-01}**. However, whether this inhibition results from a direct or an indirect blockade of this protease by alteration of the maturation process remains to be investigated. In a previous study, we observed that the pharmacological inhibition of CatC with **IcatC_{XPZ-01}** or **IcatC_{BI-9740}** in a stem cell model reduced membrane-bound PR3 more than a CatC loss-of-function mutation [19,26]. In view of the current data, the stronger membrane-bound PR3 reduction achieved with **IcatC_{XPZ-01}** or **IcatC_{BI-9740}** could be explained by the inhibition of NSPs-AAP-1.

Cell-permeable CatC inhibitors blocked the activation of proNSPs in neutrophils differentiated from progenitor cells *in vitro* [19,26,39]. As an alternative approach to the traditional targeting of CatC's active site, we used cell-permeable inhibitors (**IcatS_{#54}** or compound 1) targeting proCatC activation during the differentiation of human in CD34⁺ progenitor cells into neutrophils. This almost totally abrogated proCatC maturation and was accompanied by a significant reduction in cellular NSP content and proteolytic activities (~70 %), as opposed to the expected ~90 % reduction in NSP activities observed in PLS neutrophils [19,22]. In this regard, it is possible that *in vitro* differentiation of neutrophils may not fully recapitulate the processes occurring in the human bone marrow. For instance, the duration of promyelocytic stage or the

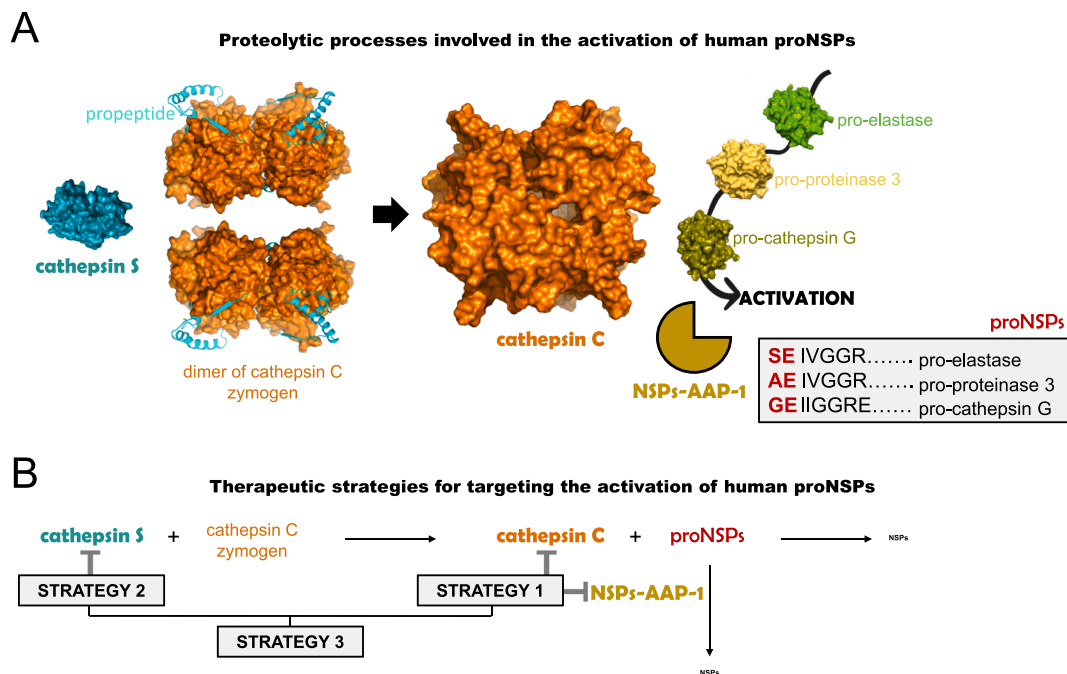


Fig. 13. Activation of proNSPs during human neutrophil differentiation. A) NSPs are synthesized in myeloblasts/promyelocytes stages of neutrophil differentiation as inactive zymogens containing a N-terminal dipropeptide in the bone marrow. Our study focusing on proteolytic pathways involved in the activation of proNSPs shows that CatS is the major protease executing proCatC maturation and NSPs-AAP-1 is an additional cysteine protease catalyzing the activation of NSPs. B) New data from the study describing in detail the proteolytic pathways implicated in the activation of proNSPs are important for the design of novel therapeutic approaches. Nitrile inhibitors which are able to inhibit CatC and NSPs-AAP-1 could better inhibit the activation of proNSPs (*therapeutic strategy 1*). CatS, a potent elastinolytic enzyme like NSPs, is a druggable major proCatC converting protease which could be targeted to prevent tissue damages in chronic inflammatory diseases. Inhibition of CatS and by consequence NSPs could be an efficient strategy to neutralize elastinolytic enzymes (*therapeutic strategy 2*). The blockade of proNSPs activation by the combination of a CatC inhibitor with a CatS inhibitor might help to improve control of tissue damage (*therapeutic strategy 3*).

expression/intracellular amounts of NSPs-AAP-1 could differ. The inability of *in vitro* differentiated human neutrophils to generate NETs also suggests that functional differences must exist [53]. Be that as it may, the combination of either **Icats**_{#54} with **IcatC**_{XPZ-01}, or of compound **1** with **IcatC**_{BI-9740}, resulted in an almost total inhibition of NSP activity and protein levels; this inhibition of NSPs-AAP-1 also took place without affecting cell differentiation. Thus, from a developmental and clinical viewpoint, nitrile type inhibitors of CatC such as **IcatC**_{XPZ-01} and **IcatC**_{BI-9740}, which display a dual activity against both CatC and NSPs-AAP-1, could be considered superior to CatC inhibitors which do not affect NSPs-AAP-1 (therapeutic strategy 1) (Fig. 13). Furthermore, our study established a new strategy to inhibit NSPs (therapeutic strategy 2) by blocking the CatC-dependent NSP activation through CatS inhibition. Finally, the combined pharmacological inhibition of CatS and CatC/NSPs-AAP-1 could provide an even more efficient inhibition of NSPs (therapeutic strategy 3), which would be particularly useful in eliminating membrane-bound PR3 in conditions like granulomatosis with polyangiitis.

CatS, which is expressed in a wide variety of immune cells, is a potent elastolytic and collagenolytic cysteine protease that retains its enzymatic activity at neutral pH, highlighting its involvement in both intra- and extracellular proteolysis. Previous work has shown that CatS is involved in the pathogenesis of several inflammatory lung diseases including chronic obstructive pulmonary disease (COPD) and cystic fibrosis [54–57]. Increased levels of CatS in patient samples correlate significantly with a decline in lung function and increased pulmonary neutrophilic infiltration [58]. Thus, pharmacological inactivation of both CatS and NSP activities (using CatS and CatC/NSPs-AAP-1 inhibitors) could more efficiently counter tissue damage in respiratory diseases. In support of this view, pharmacological inhibition or genetic depletion of CatS in mice were found to reduce inflammation and lung injury in respiratory disease models [59]. Similar observations were made in NE-deficient or in NSP triple knock-out mice [60]. To better interpret the consequences of CatS inactivation in murine disease models, we investigated its involvement in the activation of murine proNSPs. Identification of active CatC and NE (as a representative NSP) in bone marrow and blood neutrophil extracts from CatS-deficient mice showed that CatS was not essential for the activation of proNSPs in mice. Collectively, the above data support an inflammatory role for CatS itself in mouse models, insofar as it does not only rely on NSP activities. Whence the added benefit of targeting CatS in a more comprehensive anti-inflammatory therapeutic approach.

In humans we identified a CatC-independent NSP activation pathway that is catalyzed by NSPs-AAP-1. This cysteine protease could be a direct proNSP activator, like CatC, or involved in proteolytic pathways resulting in the activation of NSPs. Our *Ctsc*^{-/-} mice data suggested that an NSPs-AAP-like enzyme was also present in mice and contributed significantly to the activation of NE and PR3 (30–40 %), but not to that of CatG, during neutrophil differentiation in the bone marrow. In blood neutrophils from PLS patients, CatG is similarly much less activated (<1% versus healthy individuals) compared to NE and PR3 (<10 % versus healthy controls) [19,22]. In this regard, the glycine at P2 position in the N-terminal propeptide (Fig. 13), which is conserved in human and murine proCatG, could delay the processing and activation during neutrophil differentiation in the bone marrow. Moreover, we speculate that NSPs-AAP-1 plays a role in the activation human and murine NSP4 as the two-residue propeptides of NSP4 zymogens do not contain a glycine. In this study, we indeed observed that human and murine NSPs-AAPs were unable to cleave the fluorogenic CatC substrate, Gly-Phe-AMC, which features a glycine at P2 position. Furthermore, mouse NSPs-AAPs-1 was inhibited using **IcatC**_{XPZ-01} during *in vitro* differentiation of CatC-deficient neutrophils, resulting in the loss of NSP activation. Since both human and mouse NSPs-AAPs were inhibited by **IcatC**_{XPZ-01}, they must be largely conserved homologs. Neutrophils from CatC-deficient mice are reported to generate significantly fewer NETs than those of WT neutrophils [53], which suggests an antimicrobial role

for CatC and NSPs in health, but also raises the possibility that these proteases might contribute to chronic inflammation, given the role of NETs therein. And indeed, CatC-deficient mice are protected against experimentally induced neutrophil-mediated diseases [13]. This also reveals that the alternative proNSP activation pathway driven by NSPs-AAP-1, which generates 30–40 % of active NSPs, is insufficient to sustain neutrophil-driven diseases in CatC-deficient mice. This again illustrates the therapeutic benefit of targeting all proteases acting upstream of NSPs, including NSPs-AAP-1, CatC, and CatS.

In conclusion, we showed herein that CatS, a potent elastolytic enzyme that has been identified as a therapeutic target in chronic inflammation-associated tissue injury, is the physiologic converting protease of human neutrophilic proCatC. Pharmacological targeting of CatS using potent, cell-permeable inhibitors indeed results in a near-total blockade of proCatC maturation, accompanied by a significant inactivation and elimination of NSPs. Preventing proNSP maturation by a CatS inhibitor, alone or in combination with a CatC/NSPs-AAP-1 inhibitor, therefore represents a promising therapeutic approach to efficiently control the extent of tissue damage in neutrophil-mediated chronic inflammatory and auto-immune diseases.

5. Financial support

This work was supported by the “Ministère de l’enseignement supérieur, de la recherche et de l’innovation (MESRI)”, the “Région Centre-Val de Loire” (Project PIRANA). This project has received funding from the *European Union’s Horizon 2020 research and innovation programme* under grant agreement No 668036 (RELENT) and from Roche Pharma Research & Early Development, Roche Innovation Center Basel (Switzerland) for cathepsin C inhibition using **RO5461111**. Responsibility for the information and views set out in this study lies entirely with the authors. Ralph Kettritz was supported by grant KE 576/10-1 from the Deutsche Forschungsgemeinschaft.

CRedit authorship contribution statement

Roxane Domain: Conceptualization, Data curation, Formal analysis, Investigation, Validation, Writing – review & editing. **Seda Seren:** Conceptualization, Data curation, Formal analysis, Investigation, Writing – review & editing. **Uwe Jerke:** Data curation, Formal analysis, Investigation, Methodology, Writing – review & editing. **Manousos Makridakis:** Data curation, Formal analysis, Investigation, Methodology. **Kuan-Ju Chen:** Data curation, Formal analysis, Investigation, Methodology, Writing – review & editing. **Jérôme Zoidakis:** Data curation, Formal analysis, Investigation, Methodology, Supervision, Validation. **Moez Rhimi:** Formal analysis, Resources, Writing – review & editing. **Xian Zhang:** Data curation, Formal analysis, Investigation. **Tillia Bonvent:** Data curation, Formal analysis, Investigation. **Cécile Croix:** Data curation, Formal analysis, Investigation. **Loïc Gonzalez:** Data curation, Formal analysis, Investigation. **Dedong Li:** Data curation, Formal analysis, Investigation. **Jessica Basso:** Data curation, Formal analysis, Investigation. **Christophe Paget:** Resources, Validation. **Marie-Claude Viaud-Massuard:** Data curation, Formal analysis, Validation. **Gilles Lalmanach:** Resources, Validation. **Guo-Ping Shi:** Resources, Supervision, Validation. **Ali Aghdassi:** Resources, Validation. **Antonia Vlahou:** Validation, Writing – review & editing. **Patrick P. McDonald:** Validation, Writing – original draft. **Isabelle Couillin:** Investigation, Resources, Writing – review & editing. **Rich Williams:** Resources, Validation. **Ralph Kettritz:** Conceptualization, Validation, Writing – original draft. **Brice Korkmaz:** Conceptualization, Formal analysis, Funding acquisition, Investigation, Resources, Supervision, Validation, Writing – original draft, Writing – review & editing.

Declaration of competing interest

The authors declare the following financial interests/personal

relationships which may be considered as potential competing interests: Brice Korkmaz has been paid for the time spent as a committee member for advisory boards (Brensocatib Advisory Board (BRAB), INSMED, USA), other forms of consulting (Boehringer Ingelheim (Germany), Neuprozyme Therapeutics Aps (Denmark), Santhera Pharmaceuticals (Switzerland), Chiesi (Italy), Gerson Lehrman Group (GLG) (USA), Slingshot Insights expert network (USA)), symposium organisation (INSMED, Boehringer Ingelheim, Chiesi) and travel support, lectures or presentations, outside the submitted work. Other authors declare no competing financial interests.

Data availability

Data will be made available on request.

Acknowledgments

Brice Korkmaz acknowledges the “Alexandre von Humboldt Foundation” (Germany) for a short institutional informative visits grant (2018) and LE STUDIUM Loire Valley Institute for Advanced Studies for Research Consortium grants (2021–2022 and 2024–2025). The authors thank Dr Thibault Chazeirat (INSERM U-1100) for IC₅₀ determination, Lise Vanderlynden (INSERM U-1100) for technical assistance, and Dr Aili Lazaar from GlaxoSmithKline Pharmaceuticals for providing GSK2793660.

Data reference

List of identified proteins in 6 biological replicates of HL-60 cells. Relative abundance of proteins in each sample are presented in ppm.

<https://data.mendeley.com/datasets/tw3759s2nd/1>

References

- G.L. Burn, A. Foti, G. Marsman, D.F. Patel, A. Zychlinsky, The neutrophil, *Immunity* 54 (7) (2021) 1377–1391.
- B. Korkmaz, M.S. Horwitz, D.E. Jenne, F. Gauthier, Neutrophil elastase, proteinase 3, and cathepsin G as therapeutic targets in human diseases, *Pharmacol. Rev.* 62 (4) (2010) 726–759.
- B. Korkmaz, A. Lesner, C. Guarino, M. Wysocka, C. Kellenberger, H. Watier, U. Specks, F. Gauthier, D.E. Jenne, Inhibitors and antibody fragments as potential anti-inflammatory therapeutics targeting neutrophil proteinase 3 in human disease, *Pharmacol. Rev.* 68 (3) (2016) 603–630.
- D.E. Jenne, A. Kuhl, Production and applications of recombinant proteinase 3, wegeren’s autoantigen: problems and perspectives, *Clin. Nephrol.* 66 (3) (2006) 153–159.
- D. Turk, V. Janjic, I. Stern, M. Podobnik, D. Lamba, S.W. Dahl, C. Lauritzen, J. Pedersen, V. Turk, B. Turk, Structure of human dipeptidyl peptidase I (cathepsin C): exclusion domain added to an endopeptidase framework creates the machine for activation of granular serine proteases, *EMBO J.* 20 (23) (2001) 6570–6582.
- H.R. Gutmann, J.S. Fruton, On the proteolytic enzymes of animal tissues: an intracellular enzyme related to chymotrypsin, *J. Biol. Chem.* 174 (3) (1948) 851–858.
- V. Turk, V. Stoka, O. Vasiljeva, M. Renko, T. Sun, B. Turk, D. Turk, Cysteine cathepsins: from structure, function and regulation to new frontiers, *BBA* 1824 (1) (2012) 68–88.
- M. Cygler, J.S. Mort, Proregion structure of members of the papain superfamily. Mode of inhibition of enzymatic activity, *Biochimie* 79 (11) (1997) 645–652.
- B. Turk, D. Turk, V. Turk, Lysosomal cysteine proteases: more than scavengers, *BBA* 1477 (1–2) (2000) 98–111.
- M. Fonovic, B. Turk, Cysteine cathepsins and their potential in clinical therapy and biomarker discovery, *Proteomics Clin. Appl.* 8 (5–6) (2014) 416–426.
- M. Fonovic, B. Turk, Cysteine cathepsins and extracellular matrix degradation, *BBA* 1840 (8) (2014) 2560–2570.
- I. Dolenc, B. Turk, G. Pungercic, A. Ritonja, V. Turk, Oligomeric structure and substrate induced inhibition of human cathepsin C, *J. Biol. Chem.* 270 (37) (1995) 21626–21631.
- B. Korkmaz, G.H. Caughey, I. Chapple, F. Gauthier, J. Hirschfeld, D.E. Jenne, R. Kettritz, G. Lalmanach, A.S. Lamort, C. Lauritzen, M. Legowska, A. Lesner, S. Marchand-Adam, S.J. McKaig, C. Moss, J. Pedersen, H. Roberts, A. Schreiber, S. Seren, N.S. Thakker, Therapeutic targeting of cathepsin C: from pathophysiology to treatment, *Pharmacol. Ther.* 190 (2018) 202–236.
- S.W. Dahl, T. Halkier, C. Lauritzen, I. Dolenc, J. Pedersen, V. Turk, B. Turk, Human recombinant pro-dipeptidyl peptidase I (cathepsin C) can be activated by cathepsins L and S but not by autocatalytic processing, *Biochemistry* 40 (6) (2001) 1671–1678.
- Y. Hamon, M. Legowska, V. Herve, S. Dallet-Choisy, S. Marchand-Adam, L. Vanderlynden, M. Demonte, R. Williams, C.J. Scott, M. Si-Tahar, N. Heuze-Vourc’h, G. Lalmanach, D.E. Jenne, A. Lesner, F. Gauthier, B. Korkmaz, Neutrophilic cathepsin C is matured by a multistep proteolytic process and secreted by activated cells during inflammatory lung diseases, *J. Biol. Chem.* 291 (16) (2016) 8486–8499.
- B. Korkmaz, A. Lesner, S. Letast, Y.K. Mahdi, M.L. Jourdan, S. Dallet-Choisy, S. Marchand-Adam, C. Kellenberger, M.C. Viaud-Massuard, D.E. Jenne, F. Gauthier, Neutrophil proteinase 3 and dipeptidyl peptidase I (cathepsin C) as pharmacological targets in granulomatosis with polyangiitis (wegener granulomatosis), *Semin. Immunopathol.* 35 (4) (2013) 411–421.
- A.M. Adkison, S.Z. Raptis, D.G. Kelley, C.T. Pham, Dipeptidyl peptidase I activates neutrophil-derived serine proteases and regulates the development of acute experimental arthritis, *J. Clin. Invest.* 109 (3) (2002) 363–371.
- C. Toomes, J. James, A.J. Wood, C.L. Wu, D. McCormick, N. Lench, C. Hewitt, L. Moynihan, E. Roberts, C.G. Woods, A. Markham, M. Wong, R. Widmer, K. A. Ghaffar, M. Pemberton, I.R. Hussein, S.A. Temtamy, R. Davies, A.P. Read, P. Sloan, M.J. Dixon, N.S. Thakker, Loss-of-function mutations in the cathepsin C gene result in periodontal disease and palmoplantar keratosis, *Nat. Genet.* 23 (4) (1999) 421–424.
- S. Seren, M. Rashed Abouzaid, C. Eulenberg-Gustavus, J. Hirschfeld, H. Nasr Soliman, U. Jerke, K. N’Guessan, S. Dallet-Choisy, A. Lesner, C. Lauritzen, B. Schacher, P. Eickholz, N. Nagy, M. Szell, C. Croix, M.C. Viaud-Massuard, A. Al Farraj Aldosari, S. Raganatha, M. Ibrahim Mostafa, F. Giampieri, M. Battino, H. Cornillier, G. Lorette, J.L. Stephan, C. Goizet, J. Pedersen, F. Gauthier, D. E. Jenne, S. Marchand-Adam, I.L. Chapple, R. Kettritz, B. Korkmaz, Consequences of cathepsin C inactivation for membrane exposure of proteinase 3, the target antigen in autoimmune vasculitis, *J. Biol. Chem.* 293 (32) (2018) 12415–12428.
- Y. Hamon, M. Legowska, P. Fergelot, S. Dallet-Choisy, L. Newell, L. Vanderlynden, A. Kord Valeshabad, K. Acrich, H. Kord, T. Charalampos, F. Morice-Picard, I. Surplice, J. Zoidakis, K. David, A. Vlahou, S. Raganatha, N. Nagy, K. Farkas, M. Szell, C. Goizet, B. Schacher, M. Battino, A. Al Farraj Aldosari, X. Wang, Y. Liu, S. Marchand-Adam, A. Lesner, E. Kara, S. Korkmaz-Icoz, C. Moss, P. Eickholz, A. Taieb, S. Kavukcu, D.E. Jenne, F. Gauthier, B. Korkmaz, Analysis of urinary cathepsin C for diagnosing papillon-lefevre syndrome, *FEBS J.* 283 (3) (2016) 498–509.
- A.S. Lamort, Y. Hamon, C. Czaplowski, A. Gieldon, S. Seren, L. Coquet, F. Lecaille, A. Lesner, G. Lalmanach, F. Gauthier, D. Jenne, B. Korkmaz, Processing and maturation of cathepsin C zymogen: a biochemical and molecular modeling analysis, *Int. J. Mol. Sci.* 20 (19) (2019).
- C.T. Pham, J.L. Ivanovich, S.Z. Raptis, B. Zehnauer, T.J. Ley, Papillon-Lefevre syndrome: correlating the molecular, cellular, and clinical consequences of cathepsin C/dipeptidyl peptidase I deficiency in humans, *J. Immunol.* 173 (12) (2004) 7277–7281.
- D. Guay, C. Beaulieu, M.D. Percival, Therapeutic utility and medicinal chemistry of cathepsin C inhibitors, *Curr. Top. Med. Chem.* 10 (7) (2010) 708–716.
- N. Methot, J. Rubin, D. Guay, C. Beaulieu, D. Ethier, T.J. Reddy, D. Riendeau, M. D. Percival, Inhibition of the activation of multiple serine proteases with a cathepsin C inhibitor requires sustained exposure to prevent pro-enzyme processing, *J. Biol. Chem.* 282 (29) (2007) 20836–20846.
- B. Korkmaz, A. Lesner, M. Wysocka, A. Gieldon, M. Hakansson, F. Gauthier, D. T. Logan, D.E. Jenne, C. Lauritzen, J. Pedersen, Structure-based design and in vivo anti-arthritis activity evaluation of a potent dipeptidyl cyclopropyl nitrile inhibitor of cathepsin C, *Biochem. Pharmacol.* 164 (2019) 349–367.
- U. Jerke, C. Eulenberg-Gustavus, A. Rousselle, P. Nicklin, S. Kreideweiss, M. A. Grundl, P. Eickholz, K. Nickles, A. Schreiber, B. Korkmaz, R. Kettritz, Targeting cathepsin C in PR3-ANCA Vasculitis, *J. Am. Soc. Nephrol.* 33 (5) (2022) 936–947.
- S. Kreideweiss, G. Schanzle, G. Schnapp, V. Vintonyak, M.A. Grundl, BI 1291583: a novel selective inhibitor of cathepsin C with superior in vivo profile for the treatment of bronchiectasis, *Inflamm. Res.* (2023).
- K. Doyle, H. Lonn, H. Kack, A. Van de Poel, S. Swallow, P. Gardiner, S. Connolly, J. Root, C. Wikell, G. Dahl, K. Stenvall, P. Johannesson, Discovery of second generation reversible covalent DPP1 inhibitors leading to an oxazepane amidoacetonitrile based clinical candidate (AZD7986), *J. Med. Chem.* 59 (20) (2016) 9457–9472.
- D. Cipolla, J. Zhang, B. Korkmaz, J.D. Chalmers, J. Basso, D. Lasala, C. Fernandez, A. Teper, K.C. Mange, W.R. Perkins, E.J. Sullivan, Dipeptidyl peptidase-1 inhibition with brensocatib reduces the activity of all major neutrophil serine proteases in patients with bronchiectasis: results from the WILLOW trial, *Respir. Res.* 24 (1) (2023) 133.
- X. Chen, Y. Yan, Z. Zhang, F. Zhang, M. Liu, L. Du, H. Zhang, X. Shen, D. Zhao, J. B. Shi, X. Liu, Discovery and in vivo anti-inflammatory activity evaluation of a novel non-peptidyl non-covalent cathepsin C inhibitor, *J. Med. Chem.* 64 (16) (2021) 11857–11885.
- P. Szczesniak, M. Pieczykolan, S. Stecko, The synthesis of alpha, alpha-disubstituted alpha-amino acids via Ichikawa rearrangement, *J. Org. Chem.* 81 (3) (2016) 1057–1074.
- W. Hou, H. Sun, Y. Ma, C. Liu, Z. Zhang, Identification and optimization of novel cathepsin C inhibitors derived from EGFR inhibitors, *J. Med. Chem.* 62 (12) (2019) 5901–5919.
- K.J. Chen, J. Zhang, D. LaSala, J. Basso, D. Chun, Y. Zhou, P.P. McDonald, W. R. Perkins, D.C. Cipolla, Brensocatib, an oral, reversible inhibitor of dipeptidyl peptidase 1, mitigates interferon-alpha-accelerated lupus nephritis in mice, *Front. Immunol.* 14 (2023) 1185727.
- J.D. Chalmers, A. Gupta, S.H. Chotirmall, A. Armstrong, P. Eickholz, N. Hasegawa, P.J. McShane, A.E. O’Donnell, M. Shteinberg, H. Watz, A. Eleftheraki,

- C. Diefenbach, W. Sauter, A phase 2 randomised study to establish efficacy, safety and dosing of a novel oral cathepsin C inhibitor, BI 1291583, in adults with bronchiectasis: airleaf, ERJ Open Res 9 (3) (2023).
- [35] J.D. Chalmers, R. Kettritz, B. Korkmaz, Dipeptidyl peptidase 1 inhibition as a potential therapeutic approach in neutrophil-mediated inflammatory disease, *Front. Immunol.* 14 (2023) 1239151.
- [36] B. Korkmaz, S. Attucci, M.A. Juliano, T. Kalupov, M.L. Jourdan, L. Juliano, F. Gauthier, Measuring elastase, proteinase 3 and cathepsin G activities at the surface of human neutrophils with fluorescence resonance energy transfer substrates, *Nat. Protoc.* 3 (6) (2008) 991–1000.
- [37] B. Korkmaz, S. Attucci, E. Hazouard, M. Ferrandiere, M.L. Jourdan, M. Brillard-Bourdet, L. Juliano, F. Gauthier, Discriminating between the activities of human neutrophil elastase and proteinase 3 using serpin-derived fluorogenic substrates, *J. Biol. Chem.* 277 (42) (2002) 39074–39081.
- [38] S. Attucci, B. Korkmaz, L. Juliano, E. Hazouard, C. Girardin, M. Brillard-Bourdet, S. Rehault, P. Anthonioz, F. Gauthier, Measurement of free and membrane-bound cathepsin G in human neutrophils using new sensitive fluorogenic substrates, *Biochem. J.* 366 (Pt 3) (2002) 965–970.
- [39] C. Guarino, Y. Hamon, C. Croix, A.S. Lamort, S. Dallet-Choisy, S. Marchand-Adam, A. Lesner, T. Baranek, M.C. Viaud-Massuard, C. Lauritzen, J. Pedersen, N. Heuze-Vourc'h, M. Si-Tahar, E. Firatli, D.E. Jenne, F. Gauthier, M.S. Horwitz, N. Borregaard, B. Korkmaz, Prolonged pharmacological inhibition of cathepsin C results in elimination of neutrophil serine proteases, *Biochem. Pharmacol.* 131 (2017) 52–67.
- [40] A. Gollner, M. Koster, P. Nicklin, T. Trieselmann, E. Klein, J. Vlach, C. Heine, M. Grundl, J. Ramharter, D. Wyatt, M. Chaturvedi, A. Ciulli, K.C. Carter, S. Muller, D. Bischoff, P. Ettmayer, E. Haaksma, J. Mack, D. McConnell, D. Stenkamp, H. Weinstabl, M. Zentgraf, C.R. Wood, F. Montel, *openMe.com*: a digital initiative for sharing tools with the biomedical research community, *Nat. Rev. Drug Discov.* 21 (7) (2022) 475–476.
- [41] J.R. Wisniewski, A. Zougman, N. Nagaraj, M. Mann, Universal sample preparation method for proteome analysis, *Nat. Methods* 6 (5) (2009) 359–362.
- [42] P.E. Nikolaou, N. Mylonas, M. Makridakis, M. Makreka-Kuka, A. Iliou, S. Zerikiotis, P. Efentakis, S. Kampoukos, N. Kostomitsopoulos, R. Vilskersts, I. Ikonomidis, V. Lambadiari, C.J. Zuurbier, A. Latosinska, A. Vlahou, G. Dimitriadis, E.K. Iliodromitis, I. Andreadou, Cardioprotection by selective SGLT-2 inhibitors in a non-diabetic mouse model of myocardial ischemia/reperfusion injury: a class or a drug effect? *Basic Res. Cardiol.* 117 (1) (2022) 27.
- [43] J. Zoidakis, List of identified proteins in 6 biological replicates of HL-60 cells. Relative abundance of proteins in each sample are presented in ppm, 2023.
- [44] K.V. Rupanagudi, O.P. Kulkarni, J. Lichtnekert, M.N. Darisipudi, S.R. Mulay, B. Schott, S. Gruner, W. Haap, G. Hartmann, H.J. Anders, Cathepsin S inhibition suppresses systemic lupus erythematosus and lupus nephritis because cathepsin S is essential for MHC class II-mediated CD4 T cell and B cell priming, *Ann. Rheum. Dis.* 74 (2) (2015) 452–463.
- [45] J. Inoue, M. Nakamura, Y.S. Cui, Y. Sakai, O. Sakai, J.R. Hill, K.K. Wang, P. W. Yuen, Structure-activity relationship study and drug profile of N-(4-fluorophenylsulfonyl)-L-valyl-L-leucinal (SJA6017) as a potent calpain inhibitor, *J. Med. Chem.* 46 (5) (2003) 868–871.
- [46] I. Santamaria, G. Velasco, A.M. Pendas, A. Paz, C. Lopez-Otin, Molecular cloning and structural and functional characterization of human cathepsin F, a new cysteine proteinase of the papain family with a long propeptide domain, *J. Biol. Chem.* 274 (20) (1999) 13800–13809.
- [47] D. Bromme, K. Okamoto, Human cathepsin O2, a novel cysteine protease highly expressed in osteoclastomas and ovary molecular cloning, sequencing and tissue distribution, *Bio. Chem. Hoppe-Seyler* 376 (6) (1995) 379–384.
- [48] B.D. Gelb, G.P. Shi, M. Heller, S. Weremowicz, C. Morton, R.J. Desnick, H. A. Chapman, Structure and chromosomal assignment of the human cathepsin K gene, *Genomics* 41 (2) (1997) 258–262.
- [49] D. Bromme, Z. Li, M. Barnes, E. Mehler, Human cathepsin V functional expression, tissue distribution, electrostatic surface potential, enzymatic characterization, and chromosomal localization, *Biochemistry* 38 (8) (1999) 2377–2385.
- [50] S. Gal, M.C. Willingham, M.M. Gottesman, Processing and lysosomal localization of a glycoprotein whose secretion is transformation stimulated, *J. Cell Biol.* 100 (2) (1985) 535–544.
- [51] R. Maehr, H.C. Hang, J.D. Mintern, Y.M. Kim, A. Cuvillier, M. Nishimura, K. Yamada, K. Shirahama-Noda, I. Hara-Nishimura, H.L. Ploegh, Asparagine endopeptidase is not essential for class II MHC antigen presentation but is required for processing of cathepsin L in mice, *J. Immunol.* 174 (11) (2005) 7066–7074.
- [52] S. Kumar Vr, M.N. Darisipudi, S. Steiger, S.K. Devarapu, M. Tato, O.P. Kukarni, S. R. Mulay, D. Thomasova, B. Popper, J. Demleitner, G. Zuchriegel, C. Reichel, C. D. Cohen, M.T. Lindenmeyer, H. Liapis, S. Moll, E. Reid, A.W. Stitt, B. Schott, S. Gruner, W. Haap, M. Ebeling, G. Hartmann, H.J. Anders, Cathepsin S cleavage of protease-activated Receptor-2 on endothelial cells promotes microvascular diabetes complications, *J Am Soc Nephrol* 27 (6) (2016) 1635–1649.
- [53] H. Yan, H.F. Zhou, A. Akk, Y. Hu, L.E. Springer, T.L. Ennis, C.T.N. Pham, Neutrophil proteases promote experimental abdominal aortic aneurysm via extracellular trap release and plasmacytoid dendritic cell activation, *Arterioscler. Thromb. Vasc. Biol.* 36 (8) (2016) 1660–1669.
- [54] R. Brown, S. Nath, A. Lora, G. Samaha, Z. Elgamal, R. Kaiser, C. Taggart, S. Weldon, P. Geraghty, Cathepsin S: investigating an old player in lung disease pathogenesis, comorbidities, and potential therapeutics, *Respir. Res.* 21 (1) (2020) 111.
- [55] M.C. McKelvey, S. Weldon, D.F. McAuley, M.A. Mall, C.C. Taggart, Targeting proteases in cystic fibrosis lung disease. Paradigms, progress, and potential, *Am J Respir Crit Care Med* 201 (2) (2020) 141–147.
- [56] R. Brown, D.M. Small, D.F. Doherty, L. Holsinger, R. Booth, R. Williams, R. J. Ingram, J.S. Elborn, M.A. Mall, C.C. Taggart, S. Weldon, Therapeutic inhibition of cathepsin S reduces inflammation and mucus plugging in adult betaENaC-tg mice, *Mediators Inflamm.* 2021 (2021) 6682657.
- [57] D.F. Doherty, S. Nath, J. Poon, R.F. Foronjy, M. Ohlmeyer, A.J. Dabo, M. Salathe, M. Birrell, M. Belvisi, N. Baumlin, M.D. Kim, S. Weldon, C. Taggart, P. Geraghty, Protein phosphatase 2A reduces cigarette smoke-induced cathepsin S and loss of lung function, *Am. J. Respir. Crit. Care Med.* 200 (1) (2019) 51–62.
- [58] S. Weldon, P. McNally, D.F. McAuley, I.K. Oglesby, C.L. Wohlford-Lenane, J. A. Bartlett, C.J. Scott, N.G. McElvaney, C.M. Greene, P.B. McCray Jr., C.C. Taggart, miR-31 dysregulation in cystic fibrosis airways contributes to increased pulmonary cathepsin S production, *Am. J. Respir. Crit. Care Med.* 190 (2) (2014) 165–174.
- [59] T. Zheng, M.J. Kang, K. Crothers, Z. Zhu, W. Liu, C.G. Lee, L.A. Rabach, H. A. Chapman, R.J. Homer, D. Aldous, G.T. De Sanctis, S. Underwood, M. Graupe, R. A. Flavell, J.A. Schmidt, J.A. Elias, Role of cathepsin S-dependent epithelial cell apoptosis in IFN-gamma-induced alveolar remodeling and pulmonary emphysema, *J. Immunol.* 174 (12) (2005) 8106–8115.
- [60] N. Guyot, J. Wartelle, L. Malleret, A.A. Todorov, G. Devouassoux, Y. Pacheco, D. E. Jenne, A. Belaouaj, Unopposed cathepsin G, neutrophil elastase, and proteinase 3 cause severe lung damage and emphysema, *Am. J. Pathol.* 184 (8) (2014) 2197–2210.
- [61] R.W. Mason, G.D. Green, A.J. Barrett, Human liver cathepsin L, *Biochem. J.* 226 (1) (1985) 233–241.
- [62] J. Sage, F. Malleve, F. Barbarin-Costes, S.A. Samsonov, J.P. Gehrcke, M. T. Pisabarro, E. Perrier, S. Schnebert, A. Roget, T. Livache, C. Nizard, G. Lalmanach, F. Lecaille, Binding of chondroitin 4-sulfate to cathepsin S regulates its enzymatic activity, *Biochemistry* 52 (37) (2013) 6487–6498.
- [63] Z. Tber, M. Wartenberg, J.E. Jacques, V. Roy, F. Lecaille, D. Warszycki, A. J. Bojarski, G. Lalmanach, L.A. Agrofoglio, Selective inhibition of human cathepsin S by 2,4,6-trisubstituted 1,3,5-triazine analogs, *Bioorg. Med. Chem.* 26 (14) (2018) 4310–4319.
- [64] T. Dau, R.S. Sarker, A.O. Yildirim, O. Eickelberg, D.E. Jenne, Autoprocessing of neutrophil elastase near its active site reduces the efficiency of natural and synthetic elastase inhibitors, *Nat. Commun.* 6 (2015) 6722.